JCTC Journal of Chemical Theory and Computation

Article

pubs.acs.org/JCTC

Self-consistent Formulation of Constricted Variational Density Functional Theory with Orbital Relaxation. Implementation and Applications

Mykhaylo Krykunov and Tom Ziegler*

Department of Chemistry, University of Calgary, University Drive 2500, Calgary AB T2N-1N4, Canada

Supporting Information

ABSTRACT: We introduce here a new version of the constricted *n*th order variational density functional method (CV(n)-DFT) in which the occupied excited state orbitals are allowed to relax in response to the change of both the Coulomb and exchange-correlation potential in going from the ground state to the excited state. The new scheme is termed the relaxed self-consistent field *n*th order constricted variational density functional (RSCF-CV(n)-DFT) method. We have applied the RSCF-CV(n)-DFT scheme to the $n_\sigma \rightarrow \pi^*$ transitions in which an electron is moved from an occupied lone-pair orbital n_σ to a virtual π^* orbital. A total of 34 transitions involving 16 different compounds were considered using the LDA, B3LYP, and BHLYP functionals. The DFT-based results were compared to the "best estimates" (BE) from high level *ab initio* calculations. With energy terms included to second order in the variational parameters (CV(2)-DFT), our theory is equivalent to the adiabatic version of time dependent DFT . We find that calculated excitation energies for CV(2)-DFT using LDA and BHLYP differ substantially from BE with root-mean-square-deviations (RMSD) of 0.87 and 0.65 eV, respectively, whereas B3LYP affords an excellent fit with BE at RMSD = 0.33 eV. Resorting next to CV(∞)−DFT where energy terms to all orders in the variational parameters are included results for all three functionals in too high excitation energies with RMSD = 1.62, 1.14, and 1.48 eV for LDA, B3LYP, and BHLYP, respectively. Allowing next for a relaxation of the orbitals (n_σ,π^*) that participate directly in the transition (SCF-CV(n)-DFT) leads to an improvement with RMSD = 0.49 eV (LDA), 0.50 eV (B3LYP), and 1.12 eV (BHLYP). The best results are obtained with full relaxation of all orbitals (RSCF-CV(n)) where now RMSD = 0.61 eV (LDA), 0.32 eV (B3LYP), and 0.52 eV (BHLYP). We discuss finally the relation between RSCF-CV(n) and Slater's ΔSCF method and demonstrate that the two schemes affords quite similar results in those cases where the excitation can be described by a single orbital displacement ($n_\sigma \rightarrow \pi^*$).

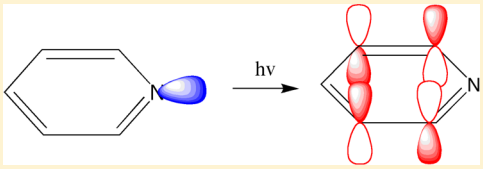

I. INTRODUCTION

Time-dependent density functional theory (TDDFT)[1−7] has become a standard method for the study of excited states. Numerous benchmark studies have shown, that excitation energies evaluated by TDDFT for transitions between orbitals of similar spatial extent such as $\pi \rightarrow \pi^*$ transitions are in satisfactory agreement with experiment. Accordingly, TDDFT has been adopted as a good compromise between rigor and computational efficiency.[8−15] However, TDDFT calculations based on the generalized gradient approximation (GGA) point to some systematic errors for transitions of electrons between two separated regions of space.[8−15] This error still persists if a fraction of Hartree−Fock exchange is added to the functional.

TDDFT is based on response theory, according to which we allow the occupied ground state Kohn−Sham orbitals to change by $\delta\psi_i$ as the result of a perturbation. The change is introduced by allowing an admixture of virtual ground state orbitals $\{\psi_a;\ a = 1,\text{vir}\}$ into ψ_i, according to

$$\psi_i = \sum_a^{\text{vir}} \tilde{U}_{ai}\psi_a \tag{1}$$

By making use of linear response theory, the transition energies are in turn evaluated to second order in U with the help of the adiabatic approximation.[1−7] We have pointed out[16,17] that the simple adiabatic linear response approach taken in TDDFT can give rise to serious errors for GGAs and other popular approximate functionals when the transitions are between orbitals of different spatial extent. We have further shown that contributions to the excitation energies up to fourth order in $\tilde{U}$ are required for a qualitatively correct description of charge transfer excitations with approximate DFT.[18,19]

In order to overcome some of the problems encountered by adiabatic TDDFT,[8−15] a new method has been introduced for the study of excited states. This theory is not time-dependent nor is it based on response theory. It is instead variational in nature and has been termed constricted variational DFT or CV(n)-DFT.[18,20,21] In CV(n)-DFT, we carry out a unitary transformation among occupied $\{\psi_i;\ i = 1,\text{occ}\}$ and virtual $\{\psi_a;\ a = 1,\text{vir}\}$ ground state orbitals

$$\tilde{Y}\begin{pmatrix}\psi_{\text{occ}}\\ \psi_{\text{vir}}\end{pmatrix} = e^{\tilde{U}}\begin{pmatrix}\psi_{\text{occ}}\\ \psi_{\text{vir}}\end{pmatrix} = \left(\sum_{m=0}^{\infty}\frac{\tilde{U}^m}{m!}\right)\begin{pmatrix}\psi_{\text{occ}}\\ \psi_{\text{vir}}\end{pmatrix} = \begin{pmatrix}\psi'_{\text{occ}}\\ \psi'_{\text{vir}}\end{pmatrix} \tag{2a}$$

Received: February 3, 2013
Published: May 16, 2013

up to $m = n$. Here, ψ_{occ} and ψ_{vir} are concatenated column vectors containing the sets of occupied $\{\psi_i; I = 1,occ\}$ and virtual $\{\psi_a; a = 1,vir\}$ ground state (reference) KS-orbitals whereas ψ'_{occ} and ψ'_{vir} are concatenated column vectors containing the resulting sets $\{\psi'_i; i = 1,occ\}$ and $\{\psi'_a; a = 1,vir\}$ of occupied and virtual excited state orbitals, respectively. The unitary transformation matrix Y is in eq 1 expressed in terms of a skew symmetric matrix $\tilde{U}$ as

$$\tilde{Y} = e^{\tilde{U}} = I + \tilde{U} + \frac{\tilde{U}^2}{2} + \cdots = \sum_{m=0}^{\infty} \frac{\tilde{U}^m}{m!} = \sum_{m=0}^{\infty} \frac{(\tilde{U}^2)^m}{2m!} + \tilde{U} \sum_{m=0}^{\infty} \frac{(\tilde{U}^2)^m}{(2n+1)!} \quad (2b)$$

Here, $\tilde{U}_{ij} = \tilde{U}_{ab} = 0$ where "i,j" refer to the occupied set $\{\psi_i; i = 1,occ\}$ whereas "a,b" refer to $\{\psi_a; a = 1,vir\}$. Further, $\tilde{U}_{ai}$ are the variational mixing matrix elements that combine virtual and occupied ground state (reference) orbitals in the excited state with $\tilde{U}_{ai} = -\tilde{U}_{ia}$. The way in which the summation in eq 2 is carried out to any desired order m is described in ref 20.

In its second order formulation (CV(2)-DFT), our theory coincides with adiabatic TDDFT when use is made of the popular Tamm−Dancoff approximation[23] within both theories. In CV(2)-DFT, we optimize $\tilde{U}_{ai}$ with respect to an energy expression that is correct to second order in $\tilde{U}$. When the summation in eq 3 is carried out to the nth order ($m = n > 2$) using the $\tilde{U}$ vector optimized from the second order energy expression, one talks about the CV(n)-DFT scheme,[20] which is a perturbational extension of CV(2)-DFT. On the other hand, the procedure in which $\tilde{U}$ is optimized from an energy expression correct to the nth order will be termed SCF-CV(n)-DFT.[21] In this nomenclature, CV(2)-DFT and SCF-CV(2)-DFT are identical. For SCF-CV(∞)-DFT, the summation in eq 3 is carried out to all orders and $\tilde{U}$ optimized with respect to the corresponding energy expression.[21]

SCF-CV(∞)-DFT bears some resemblance to ΔSCF,[24−30] predating[24−27] TDDFT. Thus, in ΔSCF a self-consistent Kohn−Sham calculation is carried out on an "excited state configuration" in which an electron has been "promoted" in energy from the ground state configuration. Thus, in those cases where the excitation can be described by a single replacement $i \rightarrow a$, ΔSCF and SCF-CV(∞)-DFT ought to give quite similar results. On the other hand, while ΔSCF is restricted to those cases, the SCF-CV(∞)-DFT method is not. Thus, as in the case of TDDFT, the SCF-CV(∞)-DFT scheme is able to deal with excitations that are described by several orbital replacements $i \rightarrow a$.

We have lately introduced the implementation[21] of the SCF-CV(∞)-DFT method in connection with calculations on a series of $\pi \rightarrow \pi^*$ transitions and demonstrated a generally good agreement with experiment for the BHLYP functional where the root mean standard deviation (RMSD) was 0.25 eV for the calculated excitation energies compared to results from high level wave function methods. It was further demonstrated that there is a good numerical agreement between SCF-CV(∞)-DFT and ΔSCF in those cases where SCF-CV(∞)-DFT describes the excitation by a single replacement.

We will in the present study report on results from SCF-CV(∞)-DFT calculations involving $n_\sigma \rightarrow \pi^*$ transitions from occupied lone-pair orbitals (n_σ) to virtual π^* orbitals. During the initial stages of our study, it became clear that calculated excitation energies based on the SCF-CV(∞)-DFT and ΔSCF methods differed considerably even in those cases where the SCF-CV(∞)-DFT scheme described the transition by a single $i \rightarrow a$ replacement. A further comparison of the SCF-CV(∞)-DFT and ΔSCF results revealed that the deviation was due to a lack of relaxation of the orbitals not participating directly in the excitations in the case of SCF-CV(∞)-DFT. We shall, as a consequence, introduce a relaxed SCF-CV(∞)-DFT scheme RSCF-CV(∞)-DFT and demonstrate that it affords results in much better agreement with ΔSCF in those cases where RSCF-CV(∞)-DFT describes the transition by a single $i \rightarrow a$ replacement. It is not surprising that relaxation is important in $n_\sigma \rightarrow \pi^*$ transitions involving orbitals of a different extent as the Coulomb potential will change drastically in going from the $(n_\sigma)^2$ ground state configuration where two electrons might be confined to a small region of space to the $(n_\sigma)^1(\pi^*)^1$ excited state configuration where the electron in π^* might be delocalized over a large region. The present study is an extension of a previous work[31] based on the perturbational CV(∞)-DFT scheme for the same excitations.

II. COMPUTATIONAL DETAILS

All calculations were based on DFT as implemented in a developers version of the ADF 2010 program.[32] Our calculations employed a standard triple-ζ Slater type orbital (STO) basis with one set of polarization functions for all atoms.[33] Use was made of the local density approximation in the VWN parametrization[34] as well as the B3LYP and BHLYP hybrid functionals by Becke,[35] with the correlation functional taken from Lee et al.[36] All electrons were treated variationally without the use of the frozen core approximation.[33] The parameter for the precision of the numerical integration was set to a (standard) value of 5.0. A special auxiliary STO basis was employed to fit the electron density in each cycle for an accurate representation of the exchange and Coulomb potentials.[33] The Cartesian coordinates of the benchmark molecules were taken from the Supporting Information of Schreiber et al.[10] The ground-state geometries of these molecules were optimized at the MP2/6-31G* level of theory.[10]

III. THEORY

Generation of Excited State Orbitals. In SCF-CV(∞)-DFT,[21] we construct excited state occupied $\{\psi'_i; i = 1,occ\}$ and virtual $\{\psi'_a; a = 1,vir\}$ KS-orbitals by performing a unitary transformation among occupied $\{\psi_i; i = 1,occ\}$ and virtual $\{\psi_a; a = 1,vir\}$ ground state orbitals and carry out the summation in eq 2b to all orders in m. For a spin conserving excitation, $\tilde{U}^{\alpha\alpha}$ generates from eq 2b the orbitals

$$\psi_q^{\alpha'} = \sum_{p}^{(occ+vir)/2} \tilde{Y}_{qp}^{\alpha\alpha} \psi_p^{\alpha} = \sum_{i}^{occ/2} \tilde{Y}_{qi}^{\alpha\alpha} \psi_i^{\alpha} + \sum_{a}^{vir/2} \tilde{Y}_{qa}^{\alpha\alpha} \psi_a^{\alpha} \quad (3a)$$

$$\psi_q^{\beta'} = \psi_q^{\beta} \quad (3b)$$

where we, without loss of generality, have assumed that the spin-conserving transition takes place in the α-manifold. Here, $\tilde{U}^{\alpha\alpha}$ and $\tilde{Y}^{\alpha\alpha}$ consist of the elements $\tilde{U}_{ai}^{\alpha\alpha}$ and $\tilde{Y}_{ai}^{\alpha\alpha}$, respectively, where a and i both refer to orbitals of α-spin. The relation between $\tilde{U}^{\alpha\alpha}$ and $\tilde{Y}^{\alpha\alpha}$ is given in ref 20.

Likewise, for a $\alpha \rightarrow \beta$ spin-flip transition, we have used $U^{\beta\alpha}$ in eq 2b,

$$\psi_q^{\alpha''} = \sum_{i}^{occ/2} \tilde{Y}_{qi}^{\beta\alpha} \psi_i^{\alpha} + \sum_{\bar{a}}^{vir/2} \tilde{Y}_{q\bar{a}}^{\beta\alpha} \psi_a^{\beta} \quad (4a)$$

$$\psi_q^{\beta''} = \psi_q^{\beta} \tag{4b}$$

$\tilde{U}^{\beta\alpha}$ and $\tilde{Y}^{\beta\alpha}$ consist of the elements $\tilde{U}_{\bar{a}i}^{\beta\alpha}$ and $\tilde{Y}_{\bar{a}i}^{\beta\alpha}$, respectively, where $\bar{a}$, here and elsewhere, refers to orbitals of β-spin and i to orbitals of α-spin. The relation between $\tilde{U}^{\beta\alpha}$ and $\tilde{Y}^{\beta\alpha}$ is given in ref 20.

Excitation Energies in RSCF-CV(∞)-DFT. For the SCF-CV(∞)-DFT scheme, all occupied β orbitals are unchanged (frozen) from the ground state, and the same is the case for a number of α orbitals that do not directly participate in the transition. To remedy this, we allow in the RSCF-CV(∞)-DFT scheme for a relaxation to second order in the mixing matrix $R_{\bar{a}\bar{i}}^{\beta\beta}$. Thus,

$$\phi_i^{\sigma}(1) \rightarrow \psi_i^{\sigma}(1) + \sum_{c}^{\mathrm{vir}/2} R_{ci}^{\sigma\sigma}\psi_c^{\sigma}(1) - \frac{1}{2}\sum_{c}^{\mathrm{vir}/2}\sum_{k}^{\mathrm{occ}/2} R_{ci}^{\sigma\sigma}R_{ck}^{\sigma\sigma}\psi_k^{\sigma}(1) + O^{(3)}[R^{\sigma}] \tag{5a}$$

$$\phi_a^{\sigma}(1) \rightarrow \psi_a^{\sigma}(1) - \sum_{k}^{\mathrm{vir}/2} R_{ak}^{\sigma\sigma}\psi_k^{\sigma}(1) - \frac{1}{2}\sum_{c}^{\mathrm{vir}/2}\sum_{k}^{\mathrm{occ}/2} R_{ak}^{\sigma\sigma}R_{ck}^{\sigma\sigma}\psi_c^{\sigma}(1) + O^{(3)}[R^{\sigma\sigma}] \tag{5b}$$

Replacing in eq 2a the matrix $\tilde{U}$ that combines occupied and virtual orbitals of the unrelaxed set $\{\psi_q;\ q = 1,\mathrm{occ} + \mathrm{vir}\}$ with the corresponding matrix U that mixes the occupied and virtual orbitals of the relaxed basis $\{\varphi_q;\ q = 1,\mathrm{occ} + \mathrm{vir}\}$ leads to the unitary transformation

$$Y\begin{pmatrix}\phi_{\mathrm{occ}}\\ \phi_{\mathrm{vir}}\end{pmatrix} = \mathrm{e}^{U}\begin{pmatrix}\phi_{\mathrm{occ}}\\ \phi_{\mathrm{vir}}\end{pmatrix} = \left(\sum_{m=0}^{\infty}\frac{U^m}{m!}\right)\begin{pmatrix}\phi_{\mathrm{occ}}\\ \phi_{\mathrm{vir}}\end{pmatrix} = \begin{pmatrix}\phi'_{\mathrm{occ}}\\ \phi'_{\mathrm{vir}}\end{pmatrix} \tag{6a}$$

in which the sets of occupied $\{\varphi_i;\ i = 1,\mathrm{occ}\}$ and virtual $\{\varphi_a;\ a = 1,\mathrm{vir}\}$ ground state (reference) KS-orbitals are converted into the resulting sets $\{\phi'_i;\ I = 1,\mathrm{occ}\}$ and $\{\phi'_a;\ a = 1,\mathrm{vir}\}$ of occupied and virtual excited state orbitals, respectively. The unitary transformation matrix Y is as in eq 2b expressed in terms of a skew symmetric matrix U as

$$Y = \mathrm{e}^{U} = I + U + \frac{U^2}{2} + \cdots = \sum_{m=0}^{\infty}\frac{U^m}{m!} = \sum_{m=0}^{\infty}\frac{(U^2)^m}{2m!} + U\sum_{m=0}^{\infty}\frac{(U^2)^m}{(2n+1)!} \tag{6b}$$

From the unitary transformation of eq 6a we obtain for a spin conserving excitation from $U^{\alpha\alpha}$

$$\phi_q^{\alpha'} = \sum_{p}^{(\mathrm{occ}+\mathrm{vir})/2} Y_{qp}^{\alpha\alpha}\phi_p^{\alpha} = \sum_{i}^{\mathrm{occ}/2} Y_{qi}^{\alpha\alpha}\phi_i^{\alpha} + \sum_{a}^{\mathrm{vir}/2} Y_{qa}^{\alpha\alpha}\phi_a^{\alpha} \tag{7a}$$

$$\phi_q^{\beta'} = \phi_q^{\beta} \tag{7b}$$

whereas $U^{\beta\alpha}$ generates

$$\phi_q^{\alpha''} = \sum_{i}^{\mathrm{occ}/2} Y_{qi}^{\beta\alpha}\phi_i^{\alpha} + \sum_{a}^{\mathrm{vir}/2} Y_{q\bar{a}}^{\beta\alpha}\phi_a^{\beta} \tag{8a}$$

$$\phi_q^{\beta''} = \phi_q^{\beta} \tag{8b}$$

We note that U and Y play the same role in RSCF-CV(∞)-DFT as $\tilde{U}$ and $\tilde{Y}$ play in SCF-CV(∞)-DFT. The only difference is that $\tilde{U}$ and $\tilde{Y}$ are matrices over the unrelaxed ground state orbitals $\{\psi_p;\ p = 1,\mathrm{occ} + \mathrm{vir}\}$, whereas U and Y are defined with respect to the relaxed reference orbitals. A detailed description of how Y can be calculated from U is given in ref 20.

Based on the generated occupied excited state orbitals, we can now obtain the corresponding densities[37,38] from which we can express the excited state energies[37,38] as a function of $U^{\sigma,\tau}$ and $R^{\sigma,\sigma}$. The excited state energies are subsequently obtained by optimizing $U^{\sigma,\tau}$ and $R^{\sigma,\sigma}$ subject to a number of constraints to be specified shortly.[37]

Starting with a spin-conserving transition, we can write the excited state energy as[21]

$$E_{\mathrm{M}} = E_{\mathrm{KS}}^{\mathrm{M}}[\rho_{\mathrm{M}}^{+}, \rho_{\mathrm{M}}^{-}] \tag{9}$$

Here,

$$\rho_{\mathrm{M}}^{+} = \rho_0^{+} + \Delta\rho_{\mathrm{M}}^{+} = 1/2\rho_0 + 1/2\Delta\rho_{\mathrm{M}} + 1/2\Delta s_{\mathrm{M}} \tag{10}$$

and

$$\rho_{\mathrm{M}}^{-} = \rho_0^{-} - \Delta\rho_{\mathrm{M}}^{-} = 1/2\rho_0 - 1/2\Delta\rho_{\mathrm{M}} - 1/2\Delta s_{\mathrm{M}} \tag{11}$$

Further, ρ_0 is the ground state density whereas $\Delta\rho_{\mathrm{M}}$ and Δs_{M} are the changes in charge and spin density, respectively, due to the excitation. We can now write the excitation energy as

$$\begin{aligned}\Delta E_{\mathrm{M}} &= E_{\mathrm{KS}}[\rho_{\mathrm{M}}^{+}, \rho_{\mathrm{M}}^{-}] - E_{\mathrm{KS}}[\rho_0^{+}, \rho_0^{-}]\\ &= \frac{1}{2}\int F_{\mathrm{KS}}^{+}\Big[\rho_0^{+} + \frac{1}{4}\Delta\rho_{\mathrm{M}} + \frac{1}{4}\Delta s_{\mathrm{M}}, \rho_0^{-} + \frac{1}{4}\Delta\rho_{\mathrm{M}} - \frac{1}{4}\Delta s_{\mathrm{M}}\Big](\Delta\rho_{\mathrm{M}} + \Delta s_{\mathrm{M}})\,\mathrm{d}\nu_1\\ &\quad + \frac{1}{2}\int F_{\mathrm{KS}}^{-}\Big[\rho_0^{+} + \frac{1}{4}\Delta\rho_{\mathrm{M}} + \frac{1}{4}\Delta s_{\mathrm{M}}, \rho_0^{-} + \frac{1}{4}\Delta\rho_{\mathrm{M}} - \frac{1}{4}\Delta s_{\mathrm{M}}\Big](\Delta\rho_{\mathrm{M}} - \Delta s_{\mathrm{M}})\,\mathrm{d}\nu_1 + O^{[3]}(\Delta\rho_{\mathrm{M}}, \Delta s_{\mathrm{M}})\end{aligned} \tag{12}$$

Here, eq 12 is derived by Taylor expanding[28] $E_{\mathrm{KS}}[\rho_{\mathrm{M}}^{+},\rho_{\mathrm{M}}^{-}]$ and $E_{\mathrm{KS}}[\rho_0^{+},\rho_0^{-}]$ from the intermediate point $(\rho_{\mathrm{Tr}}^{+},\rho_{\mathrm{Tr}}^{-}) = (\rho_0^{+} + 1/2\Delta\rho_{\mathrm{M}} + 1/2\Delta s_{\mathrm{M}}),\ (\rho_0^{-} + 1/2\Delta\rho_{\mathrm{M}} - 1/2\Delta s_{\mathrm{M}})$. Further $F_{\mathrm{KS}}^{\sigma}[\rho_{\mathrm{Tr}}^{+},\rho_{\mathrm{Tr}}^{-}]$ $(\sigma = +,-)$ is the Kohn−Sham Fock operators defined with respect to the intermediate density point $(\rho_{\mathrm{Tr}}^{+},\rho_{\mathrm{Tr}}^{-})$. The expression in eq 12 is exact to third order in $(\Delta\rho_{\mathrm{M}},\Delta s_{\mathrm{M}})$, which is usually enough. However, its accuracy can be extended to any desired order.[28]

It is tedious but straightforward to express $\Delta\rho_{\mathrm{M}}$ and Δs_{M} in terms of $U^{\alpha\alpha}$, $R^{\alpha\alpha}$, $R^{\beta\beta}$, and $\{\psi_q;\ q = 1,\mathrm{occ} + \mathrm{vir}\}$, see Sections 2.2 and 3.2 of Supporting Information (SI) S1.[37] From the formula for $\Delta\rho_{\mathrm{M}}$ and Δs_{M} given in S1 of the SI,[37] it becomes possible to express ΔE_{M} in terms of $U^{\alpha\alpha}$, $R^{\alpha\alpha}$, $R^{\beta\beta}$, and KS-type Fock matrix elements over $\{\psi_q;\ q = 1,\mathrm{occ} + \mathrm{vir}\}$, as demonstrated in Sections 2.3 and 3.3 of S1 in the SI.[37] The corresponding density expressions for a spin-flip transition are provided in Sections 2.5 and 3.5 of S1,[37] whereas the spin-flip transition energies are delineated in Sections 2.6 and 3.6 of S1.[37]

Energy Gradient Used in Optimization of *U* and *R* within RSCF-CV(∞)-DFT. We shall now illustrate how to determine R and U in such a way that $E_{\mathrm{KS}}[\rho^{+(\infty)},\rho^{-(\infty)}]$ is minimized subject to certain constraints. To this end the energy

dx.doi.org/10.1021/ct300891k | J. Chem. Theory Comput. 2013, 9, 2761−2773

gradient with respect to variations in U and R is required. Assuming that we are working on excited state number I and considering first a spin conserving transition between orbitals of α -spin, we take[21] as a starting point for $U^{\alpha\alpha}$ the Ith eigenvector $U^{(I)}$ from a TDDFT treatment in which the Tamm−Dancoff approximation[23] has been invoked (CV(2)-DFT). However, the optimization of $U^{\alpha\alpha}$ is subject to the constraint that the diagonal elements of the corresponding excited state density matrix over $\{\psi_q; q = 1,\text{occ} + \text{vir}\}$ for a spin conserving transition must satisfy.

$$\sum_{a}^{\text{vir}/2} \Delta P_{aa} = -\sum_{a}^{\text{vir}/2} \Delta P_{ii} = 1 \tag{13}$$

due to the requirement[21] that one electron must be moved from the occupied to the virtual space in the excitation. The requirement in eq 13 is met by scaling[21] $U^{(I)}$ to obtain the initial $U^{\alpha\alpha}$ as $\eta U^{(I)}$.[20] The initial $R^{\sigma\sigma}$ matrices are taken as $R^{0,\sigma\sigma}$ from first order perturbation theory, see Sections 3.4 and 3.7 of S1 in S1 (Supporting Information).[37]

Next, a Taylor expansion of $E_M = E[U^{\alpha\alpha},R^{\alpha\alpha},R^{\beta\beta}]$ from $(U^{0,\alpha\alpha},R^{0,\alpha\alpha},R^{0,\beta\beta})$ affords

$$\begin{aligned}
&E_M(U^{\alpha\alpha}, R^{\alpha\alpha}, R^{\beta\beta}) \\
&= E_M(U^{0,\alpha\alpha}, R^{0,\alpha\alpha}, R^{0,\beta\beta}) + \sum_{ai}\left(\frac{dE_M}{dU_{ai}^{\alpha\alpha}}\right)_0 \Delta U_{ai}^{\alpha\alpha} \\
&+ \sum_{\sigma}^{\alpha,\beta}\sum_{ai}\left(\frac{dE_M}{dR_{ai}^{\sigma\sigma}}\right)_0 \Delta R_{ai}^{\sigma\sigma} \\
&+ \frac{1}{2}\sum_{ai}\sum_{bi}\left(\frac{d^2E_M}{dU_{ai}^{\alpha\alpha}dU_{bj}^{\alpha\alpha}}\right)_0 \Delta U_{ai}^{\alpha\alpha}\Delta U_{bj}^{\alpha\alpha} \\
&+ \frac{1}{2}\sum_{ai}\sum_{bj}\sum_{\sigma}^{\alpha,\beta}\sum_{\tau}^{\alpha,\beta}\left(\frac{d^2E_M}{dR_{ai}^{\sigma\sigma}dR_{bj}^{\tau\tau}}\right)_0 \Delta R_{ai}^{\sigma\sigma}\Delta R_{bj}^{\tau\tau} \\
&+ \sum_{ai}\sum_{bj}\sum_{\sigma}^{\alpha,\beta}\left(\frac{d^2E_M}{dU_{ai}^{\alpha\alpha}dR_{bj}^{\sigma\sigma}}\right)_0 \Delta U_{ai}^{\alpha\alpha}\Delta R_{bj}^{\sigma\sigma} + O^{[3]}
\end{aligned} \tag{14}$$

Here, the subscript "0" indicates that the derivative is evaluated at the reference $(U^{0,\alpha\alpha}, R^{0,\alpha\alpha}, R^{0,\beta\beta})$. We can alternatively write the expansion in terms of energy gradients and energy Hessians as

$$\begin{aligned}
&E_M(U^{\alpha\alpha}, R^{\alpha\alpha}, R^{\beta\beta}) \\
&= E_M(U^{0,\alpha\alpha}, R^{0,\alpha\alpha}, R^{0,\beta\beta}) + (\Delta\vec{U}^{\alpha\alpha} \quad \Delta\vec{R}^{\alpha\alpha} \quad \Delta\vec{R}^{\beta\beta}) \\
&\times \begin{pmatrix} \vec{g}^{U^{\alpha\alpha}} \\ \vec{g}^{R^{\alpha\alpha}} \\ \vec{g}^{R^{\beta\beta}} \end{pmatrix} + \frac{1}{2}(\Delta\vec{U}^{\alpha\alpha} \quad \Delta\vec{R}^{\alpha\alpha} \quad \Delta\vec{R}^{\beta\beta}) \\
&\times \begin{pmatrix} H^{U^{\alpha\alpha},U^{\alpha\alpha}} & H^{U^{\alpha\alpha},R^{\alpha\alpha}} & H^{U^{\alpha\alpha},R^{\beta\beta}} \\ H^{R^{\alpha\alpha},U^{\alpha\alpha}} & H^{R^{\alpha\alpha},R^{\alpha\alpha}} & H^{R^{\alpha\alpha},R^{\beta\beta}} \\ H^{R^{\beta\beta},U^{\alpha\alpha}} & H^{R^{\beta\beta},R^{\alpha\alpha}} & H^{R^{\beta\beta},R^{\beta\beta}} \end{pmatrix} \begin{pmatrix} \Delta\vec{U}^{\alpha\alpha} \\ \Delta\vec{R}^{\alpha\alpha} \\ \Delta\vec{R}^{\beta\beta} \end{pmatrix} + O^{[3]}
\end{aligned} \tag{15}$$

where the expressions for the gradients $\vec{g}^{U^{\alpha\alpha}}$, $\vec{g}^{R^{\alpha\alpha}}$, $\vec{g}^{R^{\beta\beta}}$ and Hessians $\mathbf{H}^{U^{\alpha\alpha},U^{\alpha\alpha}}$, $H^{R^{\alpha\alpha},U^{\alpha\alpha}}$, etc. can be obtained by a comparison between eqs 14 and 15. Specific formula for $\vec{g}^{U^{\alpha\alpha}}$, $\vec{g}^{R^{\alpha\alpha}}$, and $\vec{g}^{R^{\beta\beta}}$ are given in Sections 2.4 and 3.4 of S1 (SI)[37] with respect to spin conserving transitions and in Sections 2.7 and 3.7 of S1 (SI)[37] for spin-flip transitions.

Optimization of *U* and R for RSCF−CV(∞−DFT). For the spin conserving transition, a differentiation of eq 15 with respect to $\Delta U^{\alpha\alpha}$ and $\Delta R^{\beta\beta}$ affords after rearrangement

$$\begin{aligned}
&\begin{pmatrix} \vec{g}^{U^{\alpha\alpha}}(0) \\ \vec{g}^{R^{\alpha\alpha}}(0) \\ \vec{g}^{R^{\beta\beta}}(0) \end{pmatrix} + \begin{pmatrix} \mathbf{H}^{U^{\alpha\alpha},U^{\alpha\alpha}}(0) & \mathbf{H}^{U^{\alpha\alpha},R^{\alpha\alpha}}(0) & \mathbf{H}^{U^{\alpha\alpha},R^{\beta\beta}}(0) \\ \mathbf{H}^{R^{\alpha\alpha},U^{\alpha\alpha}}(0) & \mathbf{H}^{R^{\alpha\alpha},R^{\alpha\alpha}}(0) & \mathbf{H}^{R^{\alpha\alpha},R^{\beta\beta}}(0) \\ \mathbf{H}^{R^{\beta\beta},U^{\alpha\alpha}}(0) & \mathbf{H}^{R^{\beta\beta},R^{\alpha\alpha}}(0) & \mathbf{H}^{R^{\beta\beta},R^{\beta\beta}}(0) \end{pmatrix} \\
&\times \begin{pmatrix} \Delta\vec{U}^{\alpha\alpha} \\ \Delta\vec{R}^{\alpha\alpha} \\ \Delta\vec{R}^{\beta\beta} \end{pmatrix} = 0
\end{aligned} \tag{16}$$

from which we can find $(\Delta\vec{U}^{\alpha\alpha}, \Delta\vec{R}^{\alpha\alpha}, \Delta\vec{R}^{\beta\beta})$ iteratively. Here, the argument "(0)" indicates that the gradients and Hessians are evaluated at $(U^{0,\alpha\alpha}, R^{0,\alpha\alpha}, R^{0,\beta\beta})$. In the initial steps where $|\Delta\vec{U}^{\alpha\alpha}|,|\Delta\vec{R}^{\alpha\alpha}| \gg \delta_{\text{tresh1}}$, the Hessian is calculated approximately by assuming that all off-diagonal Hessian elements are zero. Further, $\mathbf{H}^{U^{\alpha\alpha},U^{\alpha\alpha}}(0) = \mathbf{H}^{R^{\alpha\alpha},R^{\alpha\alpha}}(0) = \mathbf{H}^{R^{\beta\beta},R^{\beta\beta}}(0) = \varepsilon^D$, where $(\varepsilon^D)_{ai,bj} = \delta_{ab}\delta_{ij}(\varepsilon_a - \varepsilon_i)$. We thus get for each new (steepest decent) step

$$\Delta\vec{U}^{\alpha\alpha} = (\varepsilon^D)^{-1}\vec{g}^{U^{\alpha\alpha}}(0) \tag{17}$$

$$\Delta\vec{R}^{\sigma\sigma} = (\varepsilon^D)^{-1}\vec{g}^{R^{\sigma\sigma}}(0) \tag{18}$$

"ai" is in line with general conventions considered as a single running index over orbital pairs. As a consequence, $U^{\alpha\alpha}$, $R^{\sigma\sigma}$, $\Delta U^{\alpha\alpha}$, and $\Delta R^{\sigma\sigma}$ become vectors, which is indicated by a superscript "$\rightarrow$", and $\mathbf{H}$ becomes a matrix. In other cases, $U^{\alpha\alpha}$, $R^{\sigma\sigma}$, $\Delta U^{\alpha\alpha}$, and $\Delta R^{\sigma\sigma}$ are considered as matrices with two running indices "a" and "i". Here, "$\rightarrow$" is omitted.

If the matrix $\widetilde{\widetilde{U}}^{0,\alpha\alpha} = U^{0,\alpha\alpha} + \Delta U^{0,\alpha\alpha}$ does not satisfy eq 13, we introduce a scaling so that $\hat{U}^{0,\alpha\alpha} = \eta\widetilde{\widetilde{U}}^{0,\alpha\alpha}$ satisfies eq 13. With $\hat{U}^{0,\alpha\alpha}$ satisfying eq 13, we finally ensure that the matrix $\hat{U}^{0,\alpha\alpha}$ satisfy $\text{Tr}(U^{0,\alpha\alpha+}U^{k,\alpha\alpha}) = 0$ for all the excited states $K = 1,I-1$ that are below the excited state I for which we are optimizing U. This is done by introducing the projection

$$\begin{aligned}
U^{0,\alpha\alpha} = \hat{U}^{0,\alpha\alpha} - \sum_{k=1}^{l-1} U^{K,\alpha\alpha}\text{Tr}(U^{K,\alpha\alpha+}\hat{U}^{0,\alpha\alpha}) \\
/\text{Tr}(U^{K,\alpha\alpha+}U^{K,\alpha\alpha})
\end{aligned} \tag{19a}$$

where $U^{K,\alpha\alpha+}$ is the transposed of $U^{K,\alpha\alpha}$. In order to ensure that the constraint in eq 13 is not circumvented by orbital relaxation, we introduce in addition the constraint

$$\begin{aligned}
R^{0,\alpha\alpha} = \hat{R}^{0,\alpha\alpha} - \sum_{k=1}^{l-1} U^{K,\alpha\alpha}\text{Tr}(U^{K,\alpha\alpha+}\hat{R}^{0,\alpha\alpha}) \\
/\text{Tr}(U^{K,\alpha\alpha+}U^{K,\alpha\alpha})
\end{aligned} \tag{19b}$$

for $R^{0,\alpha\alpha}$. We finally require

$$R^{0,\alpha\alpha} = \hat{R}^{0,\sigma\sigma} - \sum_{k=1}^{l-1} R^{K,\sigma\sigma}\text{Tr}(U^{K,\alpha\alpha+}\hat{R}^{0,\sigma\sigma})/\text{Tr}(R^{K,\sigma\sigma+}R^{K,\sigma\sigma}) \tag{19c}$$

After that, we go back to eqs 17 and 18 followed by a new step with $U^{0,\alpha\alpha}$, $R^{0,\sigma\sigma}$ defined in eqs 19a, 19b, and 19c. When $\delta_{\text{tresh1}} < |\Delta\vec{U}^{\alpha\alpha}|, |\Delta\vec{R}^{\sigma\sigma}| \gg \delta_{\text{tresh2}}$ the iterative procedure is resumed by the help of the conjugated gradient technique described by Pople et al.[39] It is not required in this procedure explicitly to know the Hessian. Instead, use is made of the fact that

$$\begin{pmatrix} \mathbf{H}^{U^{\alpha\alpha},U^{\alpha\alpha}}(0) & \mathbf{H}^{U^{\alpha\alpha},R^{\alpha\alpha}}(0) & \mathbf{H}^{U^{\alpha\alpha},R^{\beta\beta}}(0) \\ \mathbf{H}^{R^{\alpha\alpha},U^{\alpha\alpha}}(0) & \mathbf{H}^{R^{\alpha\alpha},R^{\alpha\alpha}}(0) & \mathbf{H}^{R^{\alpha\alpha},R^{\beta\beta}}(0) \\ \mathbf{H}^{R^{\beta\beta},U^{\alpha\alpha}}(0) & \mathbf{H}^{R^{\beta\beta},R^{\alpha\alpha}}(0) & \mathbf{H}^{R^{\beta\beta},R^{\beta\beta}}(0) \end{pmatrix} \times \begin{pmatrix} \Delta\vec{U}^{\alpha\alpha} \\ \Delta\vec{R}^{\alpha\alpha} \\ \Delta\vec{R}^{\beta\beta} \end{pmatrix} = \begin{pmatrix} \vec{g}^{U^{\alpha\alpha}}(0^+) \\ \vec{g}^{R^{\alpha\alpha}}(0^+) \\ \vec{g}^{R^{\beta\beta}}(0^+) \end{pmatrix} - \begin{pmatrix} \vec{g}^{U^{\alpha\alpha}}(0) \\ \vec{g}^{R^{\alpha\alpha}}(0) \\ \vec{g}^{R^{\beta\beta}}(0) \end{pmatrix} + O^{[3]} \tag{20}$$

where (0^+) represents the reference point $(U^{\alpha\alpha} + \Delta U^{\alpha\alpha}, R^{\alpha\alpha} + \Delta R^{\alpha\alpha}, R^{\beta\beta} + \Delta R^{\beta\beta})$.

The value for δ_{tresh1} is typically 10^{-2} a.u. whereas $\delta_{\text{tresh2}} = 10^{-4}$ a.u. Convergence is obtained when the threshold δ_{tresh2} is reached. Typically, 20−30 iterations are required to reach δ_{tresh1} and 5−10 to reach δ_{tresh2}. We have also attempted more advanced Hessians for the first part of the optimization such as the one suggested by Fletcher[40] and implemented by Fischer and Almlöf.[41] However, it was found to be less robust than the simple steepest descent procedure in eqs 17 and 18. The optimization procedure outlined here for spin-conserving transitions can readily be formulated for spin-flip transitions as well.

Natural Transition Orbitals. The occupied excited state α-orbitals from a spin-conserving excitation are defined in eq 7a. They can also be written as[20]

$$\phi_i' = \cos[\gamma_i]\phi_{i_o}^{\alpha} + \sin[\gamma_i]\phi_{i_v}^{\alpha}; \quad i = 1, \text{occ}/2. \tag{21}$$

Here, $\gamma_i (i = 1,\text{occ}/2)$ is a set of eigenvalues to

$$(\mathbf{V}^{\alpha\alpha})^{+}\mathbf{U}^{\alpha\alpha}\mathbf{W}^{\alpha\alpha} = \mathbf{1}\gamma \tag{22}$$

where γ is a diagonal matrix of dimension occ/2. Further,

$$\phi_i^{o_\alpha} = \sum_j^{\text{occ}/2} (W^{\alpha\alpha})_{ji}\phi_j^{\alpha} \tag{23}$$

and

$$\phi_{i_v}^{\alpha} = \sum_a^{\text{occ}/2} (V^{\alpha\alpha})_{ai}\phi_a^{\alpha} \tag{24}$$

where i, j run over the occupied ground state orbitals and a over the virtual ground state orbitals. The orbitals defined in eqs 23 and 24 have been referred to as Natural Transition Orbitals (NTOs),[43,44] since they give a more compact description of the excitations than the canonical orbitals. Thus, a transition that involves several $i\rightarrow j$ replacements among canonical orbitals can often be described by a single replacement $\phi_{i_o}^{\alpha}\rightarrow\phi_{i_v}^{\alpha}$ in terms of NTOs. In that case $\gamma_j = \pi/2$ for $j = i$ whereas $\gamma_j = 0$ for $j \neq i$ as a consequence of the constraint given in eq 13.

For spin-flip transitions the ground state $\alpha-$ orbitals are transformed into orbitals of the form given in eq 8. They can be written in terms of NTOs as

$$\phi_i'' = \cos[\breve{\gamma}_i]\breve{\phi}_{i_o}^{\alpha} + \sin[\breve{\gamma}_i]\breve{\phi}_{i_v}^{\beta}; \quad i = 1, \text{occ}/2 \tag{25}$$

Now, $\breve{\gamma}_i (i = 1,\text{occ}/2)$ is a set of eigenvalues to

$$(\mathbf{V}^{\beta\alpha})^{+}\mathbf{U}^{\beta\alpha}\mathbf{W}^{\beta\alpha} = \mathbf{1}\gamma \tag{26}$$

where

$$\breve{\phi}_{i_o}^{\alpha} = \sum_j^{\text{occ}/2} (W^{\beta\alpha})_{ji}\breve{\phi}_j^{\alpha} \tag{27}$$

and

$$\breve{\phi}_{i_v}^{\beta} = \sum_a^{\text{vir}/2} (V^{\beta\alpha})_{ai}\breve{\phi}_a^{\beta} \tag{28}$$

Further, i,j run over the occupied ground state orbitals of α-spin and a over the virtual ground state orbitals of β-spin. We note that for each pair $(\phi_{i_o}^{\alpha}, \phi_{i_v}^{\alpha})$ of NTOs for a spin conserving transition we can find a pair $(\breve{\phi}_{i_o}^{\alpha}, \breve{\phi}_{i_v}^{\alpha})$ of NTOs from a spin-flip transition with the same eigenvalue γ_i provided that $U^{\alpha\alpha} = U^{\beta\alpha}$. In that case, for each i, $\phi_{i_o}^{\alpha}$ and $\breve{\phi}_{i_o}^{\alpha}$ have the same spatial part as have $\phi_{i_v}^{\alpha}$ and $\breve{\phi}_{i_v}^{\beta}$.

Resolution of Singlet and Triplet Transitions from a Closed Shell Molecule. Associated with each spin-conserving transition from a closed shell ground state is a Kohn−Sham determinant with two unpaired electrons of opposite spin. Such a determinant

$$\Psi_{\text{M}}' = |\phi_1'\phi_2'\phi_3'...\phi_i'\phi_j'...\phi_n'| \tag{29}$$

has an energy[32] that is half singlet and half triplet

$$E_{\text{M}}' = \frac{1}{2}[E_{\text{S}}' + E_{\text{T}}'] \tag{30}$$

On the other hand, the spin-flip transition results in a determinant

$$\Psi_{\text{T}}'' = |\psi_1''\psi_2''\psi_3''...\psi_i''\psi_j''...\psi_n''| \tag{31}$$

with the energy of a triplet, E_{T}''. We can thus get[42] the triplet energy from Ψ_{T}'' as E_{T}'' and the singlet energy E_{S}' from Ψ_{M}' as[32]

$$E_{\text{S}}' \approx 2E_{\text{M}}' - E_{\text{T}}'' = E_{\text{S}}' + (E_{\text{S}}' - E_{\text{T}}'') \tag{32}$$

Strictly speaking, E_{S}' can only be calculated from eq 32 if $E_{\text{T}}' = E_{\text{S}}''$. This will, to a good approximation, be the case[32] if all the closed shell orbitals in Ψ_{M}' and Ψ_{T}'' are the same whereas the open shell orbitals have identical spatial parts. To ensure this, we optimize $U^{\alpha\alpha}$, $R^{\sigma\sigma}$ with respect to E_{M}'. The resulting orbitals describing Ψ_{M}' are subsequently used to construct Ψ_{T}'' and evaluate $E_{\text{T}}'' = E_{\text{T}}'$ after the required spin flip for the open shell orbitals. A slightly more accurate procedure would be to optimize $U^{\alpha\alpha}$, $R^{\sigma\sigma}$ based on the energy $2E_{\text{M}}' - E_{\text{T}}''$.

Relation between CV(∞)-DFT and ΔDFT.[16] We get readily[38] from eqs 12 and 21 with the help of the Tamm−Dancoff approximation[23]

$$E_{\text{M}}' - E^0 = \Delta E_{\text{M}}^{[\infty]} = \sum_i^{\text{occ}/2} \sin^2[\eta\gamma_i]\left(\varepsilon_{i_v}\left(\rho^0 + \frac{1}{2}\Delta\rho_{\text{M}}^{[\infty]}\right) - \varepsilon_{i_o}\left(\rho^0 + \frac{1}{2}\Delta\rho_{\text{M}}^{[\infty]}\right)\right) + \sum_i^{\text{occ}/2}\sum_j^{\text{occ}/2} \sin[\eta\gamma_i] \times \cos[\eta\gamma_i]\sin[\eta\gamma_j]\cos[\eta\gamma_j]K_{i_o i_v j_o j_v} \tag{33}$$

dx.doi.org/10.1021/ct300891k | J. Chem. Theory Comput. 2013, 9, 2761−2773

A detailed derivation of this remarkably simple expression is given in in S2 of the SI.[37] In eq 33, the summation is over orbitals of α-spin.

Here, in general,

$$K_{pq,st} = K^{C}_{pq,st} + K^{XC}_{pq,st} \tag{34}$$

with

$$K^{C}_{pq,st} = \int\int \phi_p(1)\phi_q(1)\frac{1}{r_{12}}\phi_s(2)\phi_t(2)\,\mathrm{d}v_1\,\mathrm{d}v_2 \tag{35}$$

Further, $K^{XC}_{ai,bj}$ is given by

$$K^{XC(HF)}_{pq,st} = -\int\int \phi_p(1)\phi_s(1)\frac{1}{r_{12}}\phi_q(2)\phi_t(2)\,\mathrm{d}v_1\,\mathrm{d}v_2 \tag{36}$$

for Hartree−Fock exchange correlation and by

$$K^{XC(LDA)}_{pq,st} = \int \phi_p(\vec{r}_1)\phi_q(\vec{r}_1)f(\vec{r}_1)\phi_s(\vec{r}_1)\phi_t(\vec{r}_1)\,\mathrm{d}\vec{r}_1 \tag{37}$$

for LDA exchange correlation. The integration in eqs 35 and 36 is over space and spin, whereas it is over space only in eq 37. The factor $f(\vec{r}_1)$ in eq 37 represents the regular energy kernel[2,3] in those cases where ϕ_p matches the spin of ϕ_q and ϕ_s that of ϕ_t. The only other case where $K^{XC(LDA)}_{pq,st} \neq 0$ corresponds to ϕ_p and ϕ_s being of one spin and ϕ_q, ϕ_t of the other. In that case, we make use of the expression for $f(\vec{r}_1)$ derived by Wang and Ziegler from noncollinear DFT theory .[45−47]

In eq 33, $\varepsilon_{i_o}(\rho^0 + 1/2\Delta\rho^{[\infty]}_M)$ and $\varepsilon_{i_v}(\rho^0 + 1/2\Delta\rho^{[\infty]}_M)$ correspond to orbital energies of $\phi^{\alpha}_{i_o}$ and $\phi^{\alpha}_{i_v}$, respectively, with respect to a density at the midpoint (or *transition state*)[24,25] between that of the ground state and the excited state. For a transition represented by a single replacement $\phi^{\alpha}_{i_o}\rightarrow\phi^{\alpha}_{i_v}$ with $\gamma_j = \pi/2$ for $j = i$ whereas $\gamma_j = 0$ for $j \neq i$, we have[38]

$$\Delta E^{[\infty]}_M = \varepsilon_{i_v}(\rho^0 + 1/2\Delta\rho^{[\infty]}_M) - \varepsilon_{i_o}(\rho^0 + 1/2\Delta\rho^{[\infty]}_M) \tag{38}$$

This equation represents Slater's *transition state* expression[24,25] for the excitation energy involving a single spin conserving orbital replacement. The same expression can be rewritten

$$\Delta E^{[\infty]}_M = \varepsilon_{i_v}(\rho^0) - \varepsilon_{i_o}(\rho^0) + \frac{1}{2}K_{i_oi_oi_oi_o} + \frac{1}{2}K_{i_vi_vi_vi_v} - K_{i_vi_vi_oi_o} + O^{[3]}(\Delta\rho^{[\infty]}_M) \tag{39}$$

in terms of the ground state orbital energies by the help of a Taylor expansion. This is the excitation energy expression in ΔDFT[16] for a spin conserving transition involving a single orbital displacement, $\phi^{\alpha}_{i_o}\rightarrow\phi^{\alpha}_{i_v}$. In the more elaborate ΔSCF scheme, the orbitals involved are obtained from separate SCF-calculations on each excited state represented by a single orbital displacement. This corresponds to our RSCF-CV(∞)-DFT scheme with the restriction that $\gamma_j = \pi/2$ for $j = i$ whereas $\gamma_j = 0$ for $j \neq i$.

Relation between CV(∞)-DFT and TDDFT. While the ΔDFT/ΔSCF schemes are restricted to excitations involving a single orbital displacement, CV(∞)-DFT and its extensions can deal with excitations involving multiorbital displacements through the terms containing $K_{ioivjojv}$. Thus, in this respect, CV(∞)-DFT is similar to adiabatic TDDFT. In fact, adiabatic TDDFT is an approximation to CV(∞)-DFT in which relaxation is neglected ($R = 0$) and energy terms only are kept to second order in $\tilde{U}$ as in CV(2)-DFT. The resulting energy expression reads

$$E'_M - E^0 \approx \Delta E^{[2]}_M = \sum_i^{occ/2}\sum_a^{vir/2}\tilde{U}^{\alpha\alpha}_{ai}\tilde{U}^{\alpha\alpha}_{ai}[\varepsilon_a(\rho^0) - \varepsilon_i(\rho^0)] + \sum_i^{occ/2}\sum_a^{vir/2}\sum_j^{occ/2}\sum_b^{vir/2}\tilde{U}_{ai}\tilde{U}_{bj}K_{aibj} \tag{40}$$

where the summation is over virtual "a" and occupied "i" unrelaxed ground state orbitals.

We see that both $\Delta E^{[2]}_M$ of eq 31 and $\Delta E^{[\infty]}_M$ in eq 33 have a "diagonal" term containing a weighted sum of the relative energies for the various configurations $(i)(a)$ or $(\varphi_{io\alpha})(\varphi_{iv\alpha})$ in terms of orbital energy differences as well as a "off-diagonal" term accounting for the interaction between the different configurations. In adiabatic TDDFT/TD or CV(2)-DFT, the diagonal terms are only correct to second order in $\tilde{U}$ and involve just ground state orbital energy differences whereas $\Delta E^{[\infty]}_M$ contains orbital energy differences based on the *transition state*.[24,25] For the *off-diagonal* terms, the form is quite similar in $\Delta E^{[2]}_M$ and $\Delta E^{[\infty]}_M$. For excitations with many one-electron displacements the off-diagonal terms become equal since

$$\sum_i^{occ/2}\sin[\eta\gamma_i]\cos[\eta\gamma_i]\phi_{i^{o\alpha}}\phi_{i^{v\alpha}} \approx \sum_i^{occ/2}\sum_a^{vir/2}U_{ai}\phi_a\phi_i \tag{41}$$

as a consequence of the constraint in eq 13. On the other hand, for a transition with a single orbital replacement the second term in eq 33 becomes zero for CV(∞)-DFT resulting in either eq 38 or 39. This is in contrast to CV(2)-DFT where the second term in nonzero resulting in an expression for $\Delta E^{[2]}_M$ given by

$$\Delta E^{[2]}_M = \varepsilon_a(0) - \varepsilon_i(0) + K_{aiai} \tag{42}$$

We shall comment on the difference between eqs 38 and 39 on the one hand and eq 42 on the other later.

IV. RESULTS AND DISCUSSION

We present here results from calculations on 34 $n\rightarrow\pi^*$ excitations (T1) involving the 16 different compounds shown in Figure 1. Use will be made of adiabatic TDDFT within the Tamm−Dancoff approximation (TD), which is equivalent to CV(2)-DFT with TD included. We shall further employ the CV(∞)-DFT, SCF-CV(∞)-DFT, and RSCF-CV(∞)-DFT schemes as well as the ΔSCF method. Our calculations are based on LDA[34] as well as the two hybrids B3LYP[35] and BHLYP[35] with respectively 20% and 50% Hartree−Fock exchange. All the DFT results will be compared to the best estimates for the excitation energies obtained by Schreiber et al.[10] based on high level wave function calculations.

The $n_\sigma\rightarrow\pi^*$ transitions belong to a category of excitations where the attach- and detach-densities have very little overlap. Such transitions are in some cases poorly represented by TDDFT/TD or CV(2)-DFT/TD as in the case of charge transfer. We have in a previous study[33] applied CV(2)-DFT/TD and CV(∞)-DFT to the T1 benchmark in order to gauge how CV(2)-DFT/TD fares for $n_\sigma\rightarrow\pi^*$ transitions and to what degree the higher order terms in CV(∞)-DFT constitute an improvement. At that time, a self-consistent formulation of CV(∞)-DFT was lacking and the influence of orbital relaxation could only be judged in those cases where ΔSCF was applicable. With the full implementation of SCF-CV(∞)-DFT and RSCF-(∞)-DFT, we are now able to judge the influence of both U and R optimization. We shall further be able to assess to what degree results from RSCF-(∞)-DFT and ΔSCF agree in those cases where the

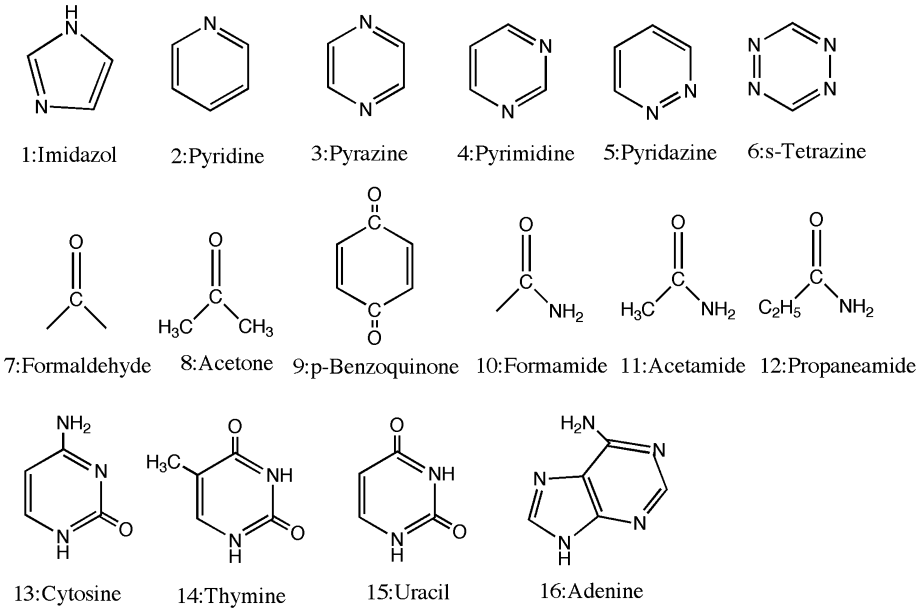

Figure 1. Molecules investigated in this study.

Table 1. Vertical Singlet Excitation Energies[a] for $n\rightarrow\pi^*$ Transitions Using LDA(VWN)

molecule	state	best[b]	CV(2)[c]	CV(∞)[c]	γ_{max}	SCF-CV(∞)[c]	γ_{max}	R-SCF-CV(∞)[c]	γ_{max}	ΔSCF
imidazole	A″	6.81	5.32	7.04	1.55	6.63	0.927	6.01	0.999	5.73
pyridine	B_1	4.59	4.30	6.30	1.57	4.99	1.571	4.66	1.571	4.58
	A_2	5.11	4.35	7.21	1.49	5.77	1.188	4.97	1.570	4.94
pyrazine	B_{3u}	3.95	3.52	3.67	1.56	3.54	1.571	3.44	1.571	3.45
	A_u	4.81	3.91	5.01	1.56	4.78	1.571	4.11	1.571	4.16
	B_{2g}	5.56	5.03	5.58	1.54	5.35	1.571	5.14	1.571	5.10
	B_{1g}	6.60	5.40	7.40	1.00	6.81	0.913	5.83	1.571	5.87
pyrimidine	B_1	4.55	3.73	4.61	1.53	4.28	1.570	3.87	1.571	3.87
	A_2	4.91	3.93	5.21	1.22	4.82	1.127	4.18	1.569	4.21
pyridazine	B_1	3.78	3.10	4.63	1.56	3.67	1.571	3.34	1.571	3.29
	A_2	4.31	3.41	5.48	1.04	4.70	0.968	3.80	1.569	3.84
	A_2	5.77	4.97	5.78	1.05	4.99	0.973	5.09	1.570	5.06
s-tetrazine	B_{3u}	2.29	1.83	2.04	1.57	1.85	1.571	1.70	1.571	1.75
	A_u	3.51	2.73	3.57	1.41	3.45	1.255	2.87	1.570	2.95
	B_{1g}	4.73	4.01	4.27	1.55	4.01	1.571	3.85	1.571	3.91
	A_u	5.50	4.55	4.78	1.41	4.49	1.260	4.45	1.570	4.50
	B_{2g}	5.20	4.72	5.03	1.47	4.86	1.570	4.77	1.570	4.82
formaldehyde	A_2	3.88	3.64	4.65	1.57	4.23	1.571	3.73	1.571	3.73
acetone	A_2	4.40	4.16	5.44	1.57	4.88	1.571	4.29	1.571	4.33
p-benzoquinone	B_{1g}	2.76	1.86	2.18	1.52	2.00	1.571	1.92	1.571	1.88
	A_u	2.77	2.00	2.62	1.56	2.40	1.571	2.19	1.571	2.11
	B_{3u}	5.64	4.29	6.36	1.37	5.38	1.151	4.69	1.569	4.67
formamide	A″	5.63	5.33	7.23	1.46	6.44	1.284	5.70	1.569	5.66
acetamide	A″	5.69	5.31	7.32	1.24	6.41	1.124	5.69	1.565	5.67
propanamide	A″	5.72	5.34	7.30	1.45	6.33	1.118	5.67	1.565	5.67
cytosine	A″	4.87	3.74	10.03	1.01	5.32	0.928	4.71	1.368	4.64
	A″	5.26	4.41	7.89	0.82	5.50	0.875	5.11	0.873	5.12
thymine	A″	4.82	4.04	6.95	1.13	5.35	1.037	4.65	1.567	4.57
	A″	6.16	4.75	9.07	0.85	5.60	0.865	5.34	0.771	6.06
uracil	A″	4.80	3.91	7.22	1.24	5.41	1.113	4.60	1.570	4.52
	A″	6.10	4.69	9.25	0.85	5.74	0.856	5.35	0.870	6.03
	A″	6.56	5.15	8.83	1.06	5.86	0.735	5.38	0.733	5.58
adenine	A″	5.12	4.22	5.78	1.47	4.98	1.239	4.43	1.570	4.47
	A″	5.75	5.00	6.04	1.41	5.41	0.983	5.14	1.530	5.16
RMSD			0.87	1.62		0.49		0.61		0.57

[a]Energies in eV. [b]Theoretical best estimates.[10] [c]Tamm-Dancoff approximation.[23]

dx.doi.org/10.1021/ct300891k | J. Chem. Theory Comput. 2013, 9, 2761−2773

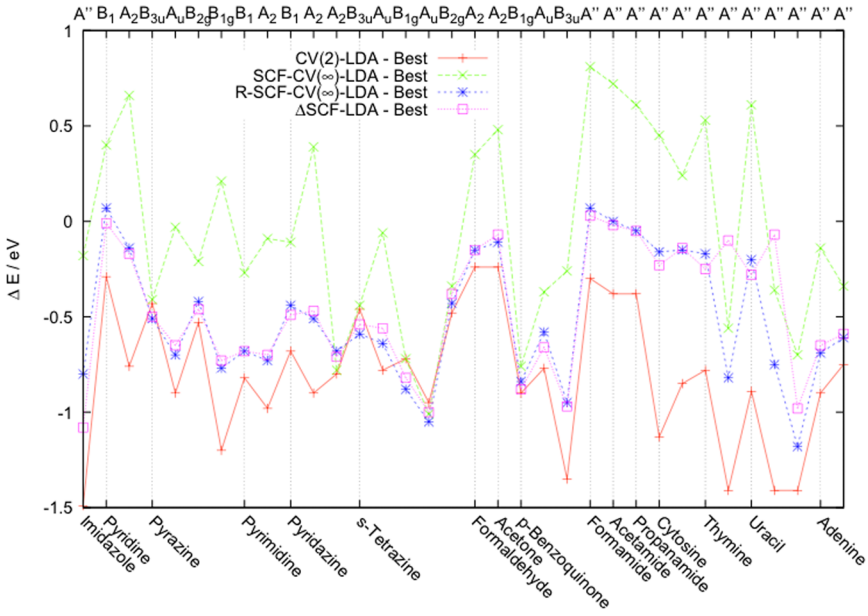

Figure 2. Differences among CV(2)-LDA, SCF-CV(∞)-LDA, RSCF-CV(∞)-LDA, ΔSCF-LDA, and best estimate.[10]

excitation under investigation can be represented by a single NTO $i \rightarrow a$ replacement.

LDA. The calculated excitation energies based on LDA are recorded in Table 1. We display further their deviation from BE[10] in Figure 2. We compare here results due to the five schemes CV(2)-DFT/TD, CV(∞)-DFT, SCF-CV(∞)-DFT, RSCF-CV(∞)-DFT, and ΔSCF with the best estimate (BE[10]) obtained from accurate wave function methods. The 34 transitions studied in Table 1 can, in full or in part, be characterized as a promotion of an electron from one $n_\sigma$orbital consisting of one or more lone-pairs situated in the plane of the molecule to a π^* orbital that is perpendicular to the plane. For those excitations in Table 1 where the largest eigenvalue (γ_{max}) from eq 22 or eq 26 is close to $\pi/2 = 1.57$, $n_\sigma \rightarrow \pi^*$ is the only contributing orbital transition. For $0.9 < \gamma_{max} < 1.5$, the dominating contribution comes from $n_\sigma \rightarrow \pi^*$, but other types of orbital transitions contribute as well. We display γ_{max} in Table 1.

The singlet excitation energy due to a pure $n_\sigma \rightarrow \pi^*$ orbital transition can in the CV(2)-DFT/TD scheme be expressed as

$$\Delta E_{S(LDA)}^{(2)(n_\sigma \rightarrow \pi^*)} = \varepsilon_{\pi^*} - \varepsilon_{n_\sigma} + 2K_{n_\sigma\pi^*,n_\sigma\pi^*} - K_{n_\sigma\bar{\pi}^*,n_\sigma\bar{\pi}^*} \quad (43)$$

according to eq 32.

It follows from Table 1 and Figure 2 that $\Delta E_{S(LDA)}^{(2)}$ underestimates the singlet excitation energies compared to BE[10] by nearly 1 eV (RMSD = 0.87 eV). Here, the major contribution to $\Delta E_{S(LDA)}^{(2)}$ [22] comes from $\Delta E_{S(LDA)}^{(2)(n_\sigma \rightarrow \pi_*)}$. Numerically, $\Delta E_{S(LDA)}^{(2)(n_\sigma \rightarrow \pi_*)}$ is dominated by $\varepsilon_{\pi^*}(0) - \varepsilon_{n\sigma}(0)$ and it is typical for LDA that $\varepsilon_{\pi^*}(0) - \varepsilon_{n\sigma}(0)$ is lower than the actual observed $i \rightarrow a$ excitation energy. The term $2K_{n_\sigma\pi^*,n_\sigma\pi^*} - K_{n_\sigma\bar{\pi}_*,n_\sigma\bar{\pi}_*}$ does also contribute to $\Delta E_{S(LDA)}^{(2)(n_\sigma \rightarrow \pi_*)}$. However, $2K_{n_\sigma\pi^*,n_\sigma\pi^*} - K_{n_\sigma\bar{\pi}_*,n_\sigma\bar{\pi}_*}$ is small as n_σ and π^* extend into different regions of space. It is typical for local functionals to underestimate $i \rightarrow a$ transition energies when a and i cover dissimilar regions of space. The most studied example is charge transfer transitions.[12] Exploratory calculations with standard local functionals based on the generalized gradient approximation (GGA) revealed that these functionals afford results quite similar in quality to LDA. A possible exception is the meta-GGA functional M06-L,[34] which for the same sample of excitations shown in Table 1 yielded a RMSD of 0.45 eV in a recent study by Jacquemin et al.[8]

The singlet excitation energy due to a pure $n_\sigma \rightarrow \pi^*$ orbital transition can in the CV(∞)-DFT/TD scheme be expressed as

$$\Delta E_{S(LDA)}^{(\infty)(n_\sigma \rightarrow \pi^*)} = \varepsilon_{\pi^*} - \varepsilon_{n_\sigma} + \frac{1}{2}K_{n_\sigma n_\sigma,n_\sigma n_\sigma} + \frac{1}{2}K_{\pi^*\pi^*,\pi^*\pi^*} - 2K_{n_\sigma n_\sigma,\pi^*\pi^*} + K_{n_\sigma n_\sigma,\bar{\pi}^*\bar{\pi}^*} \quad (44)$$

according to eqs 32 and 39.

Equations 43 and 44 are identical[27] for HF where $K_{aaaa} = K_{iiii} = 0$ and $K_{ai,ai} = -K_{aa,ii}$ for any pair (a,i).[16,17] However, for most of the popular functionals, this is not the case. Thus, the two expressions will give rise to different excitation energies for the same functional and orbitals. It follows from Table 1 that the CV(∞)-DFT excitation energies $\Delta E_{S(LDA)}^{(\infty)}$ in most cases are too large with a RMSD of 1.62 eV. The $\Delta E_{S(LDA)}^{(\infty)}$ excitation energies[22] are dominated by $\Delta E_{S(LDA)}^{(\infty)(n_\sigma \rightarrow \pi_*)}$ and the high values of $\Delta E_{S(LDA)}^{(\infty)}$ comes from $K_{\pi^*\pi^*,\pi^*\pi^*}$ and $K_{n\sigma n\sigma,n\sigma n\sigma}$ where the exchange part falls far short of canceling the positive Coulomb term. The missing cancelation has often been referred to as a self-interaction error. However, strictly speaking, $K_{aa,aa}$ or $K_{ii,ii}$ need only be zero for a one-electron system.[48]

The expression for $\Delta E_{S(LDA)}^{(\infty)(n_\sigma \rightarrow \pi_*)}$ represents, according to eq 43, the KS-energy differences

$$\Delta E_{S(LDA)}^{(\infty)(n_\sigma \rightarrow \pi^*)} = 2E^{KS}(|n_\sigma\bar{\pi}^*|) - E^{KS}(|n_\sigma\pi^*|) - E^{KS}(|n_\sigma\bar{n}_\sigma|) \quad (45)$$

Here, n_σ and π^* are natural transition orbitals (NTOs) rather than canonical ground state orbitals. However, for CV(∞) the NTOs are optimized with respect to the CV(2) energy $\Delta E_{S(LDA)}^{(2)}$ rather than $\Delta E_{S(LDA)}^{(\infty)}$.[22] The fact that the NTOs used in the energy expression for CV(∞)-DFT are not optimized with respect to $\Delta E_{S(LDA)}^{(\infty)}$ [22] might also contribute to the rather high values of the calculated CV(∞)-DFT excitation energies.

This is remedied in the SCF-CV(∞)-DFT scheme, where we now optimize $U^{\alpha\alpha}$, $U^{\beta\alpha}$ with respect to $\Delta E_{S(LDA)}^{(\infty)}$.[22] We shall give the resulting energies the special label $\Delta E_{S(LDA)}^{SCF(\infty)}$. It follows from Table 1 that the SCF-CV(∞)-DFT scheme considerably lowers

Table 2. Vertical Singlet Excitation Energies[a] in $n\rightarrow\pi^*$ Transitions Based on B3LYP

molecule	state	best[b]	CV(2)[c]	CV(∞)[c]	γ_{max}	SCF- CV(∞)[c]	γ_{max}	R-SCF-CV(∞)[c]	γ_{max}	ΔSCF
imidazole	A″	6.81	5.38	6.80	1.536	6.86	1.571	5.86	1.571	5.76
pyridine	B_1	4.59	4.92	6.01	1.509	5.34	1.571	4.91	1.571	4.69
	A_2	5.11	5.17	7.20	1.524	6.26	1.571	5.10	1.571	5.15
pyrazine	B_{3u}	3.95	4.09	4.08	1.497	3.99	1.571	3.88	1.571	3.85
	A_u	4.81	4.74	5.49	1.529	5.30	1.571	4.52	1.571	4.63
	B_{2g}	5.56	5.67	5.92	1.457	5.81	1.571	5.56	1.571	5.48
	B_{1g}	6.6	6.40	7.92	1.513	7.78	1.046	6.20	1.571	6.38
pyrimidine	B_1	4.55	4.37	4.94	1.490	4.72	1.571	4.19	1.571	4.14
	A_2	4.91	4.68	5.50	1.447	5.29	1.571	4.46	1.571	4.54
pyridazine	B_1	3.78	3.74	4.50	1.500	3.99	1.571	3.64	1.571	3.55
	A_2	4.31	4.26	5.75	1.491	5.29	1.568	3.96	1.571	4.15
	A_2	5.77	5.55	5.93	1.492	5.67	1.568	5.44	1.571	5.35
s-tetrazine	B_{3u}	2.29	2.41	2.43	1.503	2.30	1.571	2.11	1.571	2.15
	A_u	3.51	3.59	4.13	1.468	4.02	1.570	3.38	1.571	3.48
	B_{1g}	4.73	4.88	4.89	1.463	4.73	1.571	4.53	1.571	4.56
	A_u	5.5	5.20	5.22	1.454	5.16	1.570	4.92	1.571	4.96
	B_{2g}	5.2	5.40	5.34	1.474	5.31	1.571	5.16	1.571	5.17
formaldehyde	A_2	3.88	3.93	4.53	1.546	4.30	1.571	3.53	1.571	3.52
acetone	A_2	4.4	4.41	5.19	1.525	4.84	1.571	4.01	1.571	4.02
p-benzoquinone	B_{1g}	2.76	2.54	2.78	1.417	2.62	1.571	2.52	1.571	2.40
	A_u	2.77	2.69	3.15	1.406	2.97	1.571	2.72	1.571	2.55
	B_{3u}	5.64	5.47	6.82	1.496	6.18	1.568	5.40	1.571	5.40
formamide	A″	5.63	5.58	6.85	1.502	6.42	1.571	5.32	1.571	5.28
acetamide	A″	5.69	5.59	6.94	1.507	6.43	1.571	5.33	1.571	5.31
propanamide	A″	5.72	5.60	6.94	1.503	6.37	1.571	5.33	1.571	5.34
cytosine	A″	4.87	4.78	7.56	1.507	5.90	1.571	4.92	1.571	4.83
	A″	5.26	5.17	7.32	1.446	6.43	1.002	5.58	1.460	-[d]
thymine	A″	4.82	4.74	6.75	1.496	5.73	1.571	4.78	1.571	4.59
	A″	6.16	5.63	6.66	1.497	6.64	0.945	5.96	1.570	5.82
uracil	A″	4.8	4.66	6.83	1.495	5.74	1.571	4.75	1.571	4.54
	A″	6.1	5.75	8.03	1.144	6.75	0.734	5.84	1.280	6.07
	A″	6.56	5.85	6.88	1.454	6.76	0.792	6.15	1.569	-[d]
adenine	A″	5.12	5.01	5.86	1.468	5.52	1.571	4.85	1.571	4.91
	A″	5.75	5.49	6.66	1.451	6.02	1.562	5.80	1.571	5.63
RMSD			0.33	1.14		0.50		0.32		0.32

[a]Energies in eV. [b]Theoretical best estimates are from ref 10. [c]Tamm−Dancoff approximation.[23] [d]Did not converge.

the calculated excitation energies, in some cases by more that 1 eV. The RMSD in comparison to BE[10] is now 0.49 eV. The n_σ NTO representing the lone pair is quite similar for the CV(2) and SCF-CV(∞) optimizations. On the other hand, the π^* NTO involves somewhat different combinations of canonical π^* orbitals in the two cases. It is worth noting that $\Delta E^{SCF(\infty)}_{S(LDA)}$ gives rise to a considerable lowering compared to $\Delta E^{(\infty)}_{S(LDA)}$ in those compounds (1,2, and 10−15 of Table 1) where $\Delta E^{(\infty)}_{S(LDA)}$ is considerably higher than $\Delta E^{(2)}_{S(LDA)}$ whereas the corresponding stabilization is much smaller for those compounds (3,6,9 of Table 1) where $\Delta E^{(\infty)}_{S(LDA)}$ and $\Delta E^{(2)}_{S(LDA)}$ are quite similar. The first class of molecules have n_σ orbital localized on a single center with large values for $K_{n\sigma n\sigma,n\sigma n\sigma}$ whereas the second class has the n_σ lone pair orbital delocalized on 2 to 4 centers.

For those cases where SCF-CV(∞)-DFT affords $\gamma_{max} \approx \pi/2$, it is interesting to compare our SCF-CV(∞) results with the ΔSCF excitation energies $\Delta E^{\Delta SCF}_{S(LDA)}$ also given in Table 1. One might have expected the $\Delta E^{\Delta SCF}_{S(LDA)}$ and $\Delta E^{SCF(\infty)}_{S(LDA)}$ for $\gamma_{max} \approx \pi/2$ should be quite similar as both schemes in that case describe the excitation as a one orbital transition $n_\sigma\rightarrow\pi^*$ with an excitation energy given by eq 39. An inspection of Table 1 reveals that $\Delta E^{\Delta SCF}_{S(LDA)}$ consistently is lower than $\Delta E^{SCF(\infty)}_{S(LDA)}$ by between 0.5 and 1.0 eV. The reason for this deviation is that ΔSCF optimizes both the orbitals (n_σ,π^*) involved in the $n_\sigma\rightarrow\pi^*$ excitation as well as the (inactive) occupied orbitals of which those of β-spin holds half of the electrons. The inactive orbitals are not directly involved in the excitation. Nevertheless, they will relax in response to the change from the $(n_\sigma)^2$ ground state configuration to the $(n_\sigma)^1(\pi^*)^1$ excited state configuration. In the SCF-CV(∞)-DFT scheme the inactive orbitals of the excited state are all optimized with respect to the ground state. The lack of relaxation among the inactive orbitals is also a feature of CV(n)-DFT and TDDFT.

The relaxation of the inactive orbitals is taken into account to second order in the RSCF-CV(∞)-DFT scheme described. The $\Delta E^{RSCF(\infty)}_{S(LDA)}$ excitation energies calculated by this method are given in Table 1. We see that $\Delta E^{RSCF(\infty)}_{S(LDA)}$ is considerably reduced compared to $\Delta E^{SCF(\infty)}_{S(LDA)}$ due to the second order relaxation of the inactive orbitals. Further, $\Delta E^{RSCF(\infty)}_{S(LDA)}$ compares much better with $\Delta E^{\Delta SCF}_{S(LDA)}$ than $\Delta E^{SCF(\infty)}_{S(LDA)}$. We observe that the relaxation is larger for compounds (10−12) where n is localized on a single atom. This is understandable since the change in configuration from $(n_\sigma)^2$ to $(n_\sigma)^1(\pi^*)^1$ in those cases are associated with a large change in the Coulomb potential. On the other hand, the orbital relaxation energy $\Delta E^{SCF(\infty)}_{S(LDA)} - \Delta E^{RSCF(\infty)}_{S(LDA)}$ is not as large for

dx.doi.org/10.1021/ct300891k | J. Chem. Theory Comput. 2013, 9, 2761−2773

Table 3. Vertical Singlet Excitation Energies[a] for $n\rightarrow\pi^*$ Transitions Based on BHLYP

molecule	state	best[b]	CV(2)[c]	CV(∞)[c]	λ_{max}	SCF-CV(∞)[c]	λ_{max}	R-SCF-CV(∞)[c]	λ_{max}	ΔSCF
imidazole	A″	6.81	5.69	5.60	1.398	6.94	1.571	5.82	1.571	5.73
pyridine	B_1	4.59	5.43	6.18	1.474	5.80	1.571	4.79	1.571	4.76
	A_2	5.11	6.10	7.44	1.469	6.89	1.571	5.35	1.571	5.29
pyrazine	B_{3u}	3.95	4.56	5.07	1.379	4.65	1.571	4.37	1.571	4.40
	A_u	4.81	5.65	6.33	1.467	6.05	1.571	5.30	1.571	5.23
	B_{2g}	5.56	6.17	7.12	1.259	6.54	1.571	6.04	1.571	6.07
	B_{1g}	6.60	7.46	7.58	1.334	-[d]	-[d]	6.88	1.397	7.06
pyrimidine	B_1	4.55	4.99	5.80	1.389	5.37	1.571	4.54	1.571	4.51
	A_2	4.91	5.48	6.21	1.454	5.93	1.571	5.01	1.571	4.98
pyridazine	B_1	3.78	4.28	4.87	1.437	4.49	1.571	3.85	1.571	3.89
	A_2	4.31	5.13	6.46	1.304	5.93	1.571	4.37	1.571	4.44
	A_2	5.77	6.17	6.69	1.315	6.27	1.571	5.74	1.571	5.73
s-tetrazine	B_{3u}	2.29	2.91	3.36	1.408	2.96	1.571	2.59	1.571	2.65
	A_u	3.51	4.50	5.21	1.414	4.85	1.571	4.21	1.571	4.19
	B_{1g}	4.73	5.52	6.44	1.203	5.72	1.571	5.36	1.571	5.43
	A_u	5.50	5.79	6.31	1.366	5.91	1.571	5.53	1.571	5.55
	B_{2g}	5.20	5.96	6.77	1.248	6.13	1.571	5.75	1.571	5.78
formaldehyde	A_2	3.88	4.10	4.71	1.528	4.46	1.571	3.41	1.571	3.32
acetone	A_2	4.40	4.66	5.36	1.513	5.05	1.571	3.96	1.571	3.85
p-benzoquinone	B_{1g}	2.76	3.19	4.27	1.232	3.59	1.571	3.18	1.571	3.17
	A_u	2.77	3.35	4.64	1.206	3.97	1.571	3.31	1.571	3.27
	B_{3u}	5.64	6.85	7.71	1.337	7.27	1.571	6.50	1.571	6.44
formamide	A″	5.63	5.84	6.85	1.517	6.53	1.571	5.13	1.571	5.01
acetamide	A″	5.69	5.92	6.96	1.510	6.60	1.571	5.19	1.571	5.08
propanamide	A″	5.72	5.93	6.96	1.505	6.58	1.571	5.21	1.571	5.11
cytosine	A″	4.87	5.70	6.91	1.439	6.46	1.571	4.95	1.571	5.60
	A″	5.26	6.03	6.87	1.378	6.86	1.571	5.86	1.571	5.86
thymine	A″	4.82	5.40	6.64	1.476	6.16	1.571	4.47	1.571	4.44
	A″	6.16	6.16	7.11	1.438	7.21	1.571	6.14	1.571	5.96
uracil	A″	4.80	5.36	6.64	1.478	6.16	1.571	4.45	1.571	4.40
	A″	6.10	6.39	7.36	1.419	7.26	1.571	5.78	1.571	6.19
	A″	6.56	6.67	7.96	1.419	7.52	1.559	6.01	1.550	-[d]
adenine	A″	5.12	5.87	6.69	1.361	6.30	1.571	5.44	1.571	5.44
	A″	5.75	6.12	7.03	1.295	6.98	1.571	6.11	1.570	5.87
RMSD			0.65	1.48		1.12		0.44		0.48

[a]Energies in eV. [b]Theoretical best estimates.[10] [c]Tamm-Dancoff approximation.[23] [d]Did not converge.

compounds such as 6 where n_σ is delocalized over 2 to 4 centers and the change in the Coulomb potential associated with the excitation is much smaller. We note finally that the number of excitations with $\gamma_{max} \approx \pi/2$ has increased in going from SCF-CV(∞)-DFT to RSCF-CV(∞)-DFT. For the few remaining cases that involve the thymine and uracil molecules the $\Delta E^{RSCF(\infty)}_{S(LDA)}$ energies are lower than $\Delta E^{\Delta SCF}_{S(LDA)}$ as one must expect from a variational point of view. Thus, the RSCF-CV(∞)-DFT scheme incorporates ΔSCF with a single orbital transition in those cases where this is the solution with the lowest energy. However, it can also afford descriptions with several orbital transitions in those cases where such a solution is below that of ΔSCF in energy.

B3LYP and BHLYP. The excitation energies for the two hybrid functionals are shown in Table 2 for B3LYP and in Table 3 for BHLYP. The corresponding deviations from BE[10] are displayed in Figure 3 (B3LYP) and Figure 4 (BHLYP). In the case of the CV(2)-DFT scheme, there is an increase in the excitation energies from LDA to BHLYP as the fraction of exact exchange increase and the orbital difference $n_\sigma\rightarrow\pi^*$ becomes larger. Thus, on average, $\Delta E^{(2)}_{S(B3LYP)}$ is just below that of BE[10] with a RMSD of 0.33 eV whereas $\Delta E^{(2)}_{S(BHLYP)}$ is too large with RMSD = 0.65 eV. For CV(2)-DFT, we find the smallest deviation for B3LYP among the three functional investigated here. We should note that the M06 functional by Zhao and Truhlar[49,50] with 27% HF-exchange for the sample of excitations in Table 1 affords[8] RMSD = 0.24 eV.

In the case of CV(∞)-DFT, we note again an increase in the calculated excitation energies compared to CV(2)-DFT. However, the increase has diminished for the hybrids as only the local BLYP component of B3LYP (80%) and BHLYP (50%) contributes. The CV(∞)-DFT energies $\Delta E^{CV(\infty)}_{S(B3LYP)}$ and $\Delta E^{CV(\infty)}_{S(BHLYP)}$ are both too high with RMSDs of 1.14 and 1.48 eV, respectively. The orbitals used to calculate the excited state energy in the CV(∞)-DFT method are not optimal. It is thus not surprising that the excitation energies are too high. We must in general expect CV(∞)-DFT to be inadequate if the excited state Coulomb potential V^{Ex}_C differ substantially from that of the ground state, V^{Gr}_C. The $\pi\rightarrow\pi^*$ transitions in large conjugated dyes such as acenes represent cases where V^{Ex}_C and V^{Gr}_C are similar and the orbital relaxation minimal as π and π^* are equally delocalized. In such cases, already the CV(∞)-DFT method provides[22] results in good agreement with experiment and of a higher accuracy than CV(2)-DFT.[22] Subsequently optimizing n_σ,π^* in SCF-CV(∞)-DFT and the inactive orbitals in RSCF-CV(∞)-DFT brings the calculated excitation energies close to those

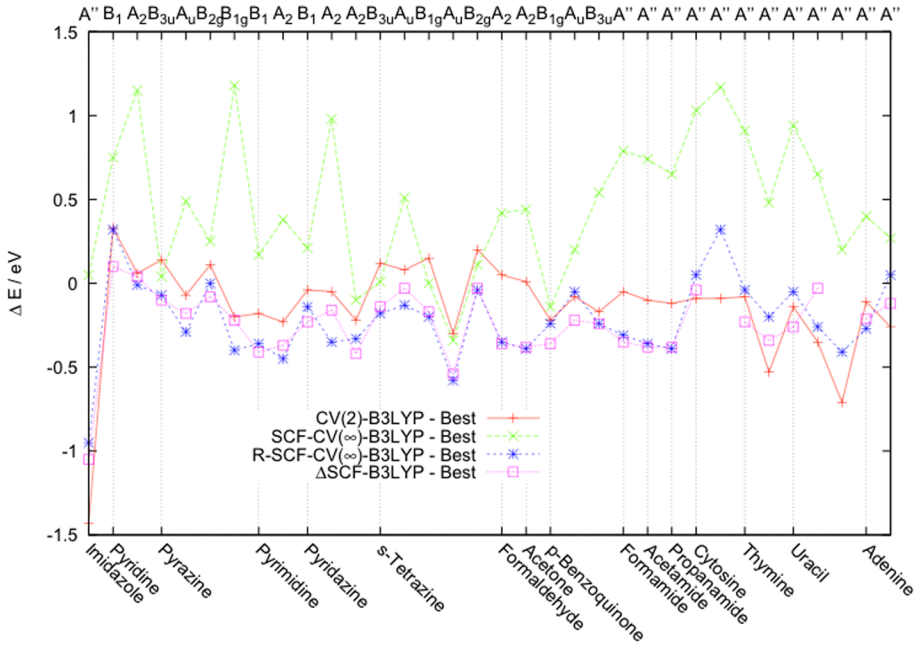

Figure 3. Difference between CV(2)-B3LYP, SCF-CV(∞)-B3LYP, RSCF-CV(∞)-B3LYP, ΔSCF-B3LYP, and best estimate.[10]

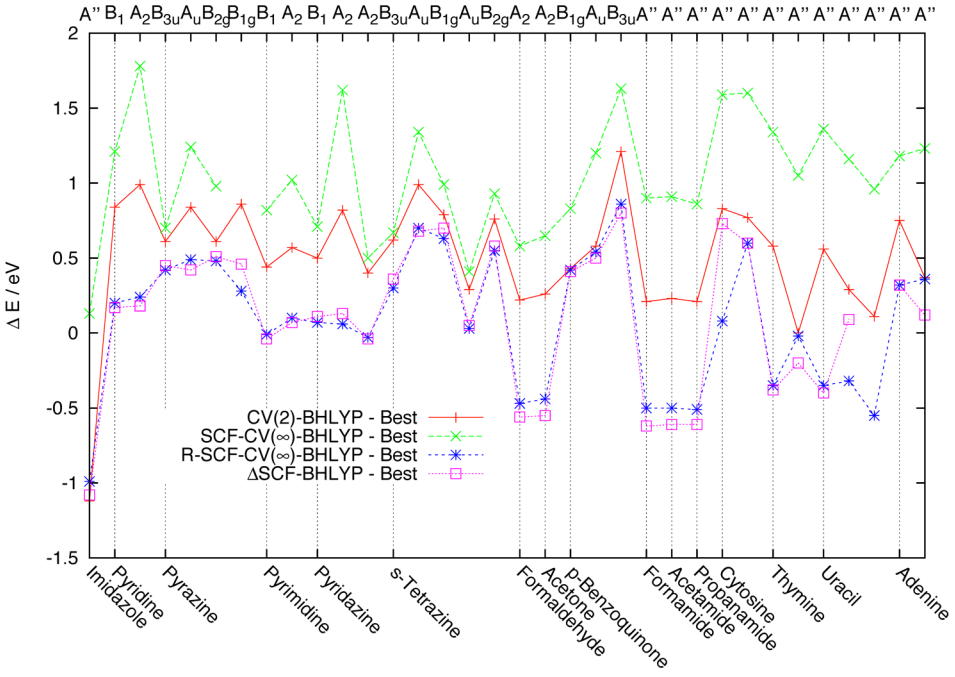

Figure 4. Difference between CV(2)-BHLYP, SCF-CV(∞)-BHLYP, RSCF-CV(∞)-BHLYP, ΔSCF-BHLYP, and best estimate.[10]

obtained as $\Delta E^{\Delta SCF}_{S(B3LYP)}$ and $\Delta E^{\Delta SCF}_{S(BHLYP)}$. However, we note in a few instances deviations between $\Delta E^{RSCF(\infty)}_{S(BHLYP)}$ and $\Delta E^{\Delta SCF}_{S(BHLYP)}$ as large as 0.2 eV in cases where $\gamma_{max} \approx \pi/2$. In terms of accuracy, ΔSCF and RSCF-CV(∞)-DFT afford the best agreement with BE[10] for B3LYP where RMSD = 0.32 eV. We have not attempted to minimize the RMSD by optimizing the fraction of exact exchange used in the ΔSCF and RSCF-CV(∞)-DFT calculations.

V. CONCLUDING REMARKS

In wave function quantum mechanics excited states have been studied either by response theory based on an exact ground state wave function or by a variational optimization of the excited state wave function.[7] In DFT, the response route in the form of time dependent DFT has been the approach of choice.[1−6] This is understandable because DFT essentially is a ground state theory. To date routine applications of TDDFT all make use of the adiabatic approximation[1−6] (AD-TDDFT) in which the energy kernel is frequency independent and practical methods beyond AD-TDDFT have not yet emerged after the formulation of AD-TDDFT some 20 years ago. We have recently taken a variational DFT approach to excited states inspired by the work of Slater and others[24−30] in order to develop a DFT based theory for excited states that goes beyond AD-TDDFT.

In our constricted variational density functional theory (CV-DFT),[18,20,21] we construct excited state KS-determinants $\Psi_I = |\phi'_1\phi'_2.....\phi'_i\phi'_j.....\phi'_n|$ from KS-orbitals that are generated by

dx.doi.org/10.1021/ct300891k | J. Chem. Theory Comput. 2013, 9, 2761−2773

the unitary transformation defined in eq 1. In this transformation occupied $\{\phi_i';i = 1,\text{occ}\}$ and virtual $\{\phi_a;i = 1,\text{vir}\}$ ground state orbitals are mixed through the transformation matrix U with the general element U_{ai}. Subsequently, U is optimized variationally with respect to the KS-energy based on Ψ_I.

At the CV(2)-DFT level of theory we express the KS-energy $E_S^{(2)}$ based on Ψ_I to second order in U and optimize U_{ai} variationally. At this simple level of CV-DFT theory, we recover within the Tamm−Dancoff approximation[18,20,21] AD-TDDFT. Following previous investigations,[12,13] it was shown in our recent studies on $\pi_A \rightarrow \pi_B^*$ charge transfer transitions[16,17,19] that the energy expression ($\Delta E_S^{(2)} = E_0 - E_S^{(2)}$) for CV(2)-DFT or AD-TDDFT is unable even qualitatively to describe charge transfer transition energies. Further, for such transitions $\Delta E_S^{(2)}$ leads to a severe underestimation of the excitation energies. In the case of the $n_\sigma \rightarrow \pi^*$ type of transitions, the error for $\Delta E_S^{(2)}$ is much smaller, and for B3LYP, we find as previously[31,51] that $\Delta E_{S(\text{B3LYP})}^{(2)}$ is in close agreement with BE[10] leading to a RMSD of only 0.33 eV.

A first step beyond the CV(2)-DFT or AD-TDDFT approach would be to calculate the KS-energy based on Ψ_I to all orders in U using the U_{ai} matrix elements optimized from CV(2)-DFT. This perturbational approach is termed CV(∞)-DFT, and the corresponding energy is given as $\Delta E_S^{(\infty)}$. For the charge transfer transitions $\pi_A \rightarrow \pi_B^*$, the inclusion of energy terms to all orders in U (CV(∞)−DFT) leads to a qualitatively correct energy expression[16,17,19] $\Delta E_S^{(\infty)}$, which contains the "self-interaction" terms $K_{\pi_A\pi_A,\pi_A\pi_A}$, $K_{\pi_B^*\pi_B^*,\pi_B^*\pi_B^*}$ and has the right asymptotic behavior as a function of the distance R_{AB} between the two fragments A and B. However, quantitatively, the calculated $\Delta E_S^{(\infty)}$ values are too high, and this is also the case for the previous[31,51] and current study of the $n_\sigma \rightarrow \pi^*$ transitions for all three functionals.

A further improvement was obtained by moving away from the perturbational approach taken in CV(∞)−DFT and optimize U with respect to the KS-energy based on Ψ_I to all orders in U. This is done in SCF-CV(∞)-DFT. It follows from Tables 1−3 and Figures 2−4 that the agreement with BE[10] now is much enhanced. Thus, the SCF-CV(∞)-DFT scheme considerably lowers the calculated excitation energies, in some cases by more that 1 eV. The stabilization comes primarily from a relaxation of the π^* NTO orbital in the $n_\sigma \rightarrow \pi^*$ transition.

The final optimization can be achieved in RSCF(∞)-CV-DFT by relaxing all the inactive orbitals that do not participate directly in the $n_\sigma \rightarrow \pi^*$ transition. This relaxation is a response to the change in the Coulomb potential as the electronic configuration goes from $(n_\sigma)^2$ in the ground state to $(n_\sigma)^1(\pi^*)^1$ in the excited state. With RSCF(∞)-CV-DFT, the deviation from BE[10] is reduced considerably. The best result is obtained for B3LYP where the RMSD now is 0.32 eV. We note further that the RSCF(∞)-CV-DFT and ΔSCF results are quite similar for the cases with $\gamma_{\max} \approx \pi/2$.

In CV-DFT, we use approximate ground state functionals in a variational description of the excited states. Such a procedure is consistent with AD-TDDFT in that this theory is equivalent to CV(2)-DFT within the TD-approximation. Going beyond the adiabatic approximation by introducing frequency dependent kernels consistent with the approximate ground state functional in TDDFT has proven difficult. Here, we go beyond CV(2)-DFT in a variational approach still using an approximate ground state functional but introducing an optimization of U based on the KS-energy of Ψ_I to all orders in U as well as relaxation of the inactive orbitals. It is hoped that going beyond CV(2) in this way will be equivalent to introducing a frequency dependent kernel in TDDFT. Obviously, with such a kernel inactive orbitals would be different from those of the ground state and vary between excited states as in the RSCF-CV(∞) scheme. Further, with a frequency dependent kernel and related Hessian, the U matrix obtained for each excited state should be different from that determined by the ground state Hessian in AD-TDDFT, just as in the SCF-CV(∞)-DFT scheme.

It can be argued that our best scheme in the form of RSCF(∞)-CV-DFT-B3LYP with RMSD = 0.32 eV only performs marginally better than the much simpler CV(2)-DFT-B3LYP method with RMSD = 0.33 eV for $n_\sigma \rightarrow \pi^*$ transition. However, we have reasons to believe[19] that our scheme also will work for charge transfer transitions where CV(2)-DFT and AD-TDDFT fail. Also, results from applications of AD-TDDFT to transition metal complexes have been mixed with many systematic errors. We hope to improve on that with the relaxation of the U matrix and the inactive orbitals. Such relaxations ought also to provide more accurate excited state properties other than the energies.

■ ASSOCIATED CONTENT

Supporting Information

S1: Formulation of the RSCF-CV(∞) scheme. S2: The energy to all orders in U for the triplet and mixed state based on corresponding orbitals with second order and all orders relaxation. This information is available free of charge via the Internet at http://pubs.acs.org

■ AUTHOR INFORMATION

Corresponding Author

*E-mail: ziegler@ucalgary.ca.

Notes

The authors declare no competing financial interest.

■ ACKNOWLEDGMENTS

T.Z. would like to thank the Canadian government for a Canada research chair in theoretical inorganic chemistry and NSERC for financial support.

■ REFERENCES

(1) Runge, E.; Gross, E. K. U. *Phys. Rev. Lett.* **1984**, *52*, 997.
(2) Casida, M. E. In *Recent Advances in Density Functional Methods*; Chong, D. P., Ed.; World Scientific: Singapore, 1995; pp 155−193.
(3) van Gisbergen, S. J. A.; Snijders, J. G. *J. Chem. Phys.* **1995**, *103*, 9347.
(4) Petersilka, M.; Grossmann, U. J.; Gross, E. K. U. *Phys. Rev. Lett.* **1996**, *76*, 12.
(5) Bauernschmitt, R.; Ahlrichs, R. *Chem. Phys. Lett.* **1996**, *256*, 454.
(6) Stratmann, R. E.; Scuseria, G. E.; Frisch, M. J. *J. Chem. Phys.* **1998**, *109*, 8218.
(7) Jensen, F. *Introduction to Computational Chemistry*; Wiley: New York, 2006; p 553.
(8) Jacquemin, D.; Perpete, E. A.; Ciofini, I.; Adamo, C.; Valero, R.; Zhao, Y.; Truhlar, D. G. *J. Chem. Theory Comput.* **2010**, *6*, 2071.
(9) Goerigk, L.; Grimme, S. *J. Chem. Phys.* **2010**, *132*, 184103.
(10) Schreiber, M.; Silva-Junior, M.; Sauer, S.; Thiel, W. *J. Chem. Phys.* **2008**, *128*, 134110.
(11) (a) Tawada, Y.; Tsuneda, T.; Yanagisawa, S.; Yanai, T.; Hirao, K. *J. Phys. Chem.* **2004**, *120*, 8425. (b) Song, J-W; Watson, M. A.; Hirao, K. *J. Chem. Phys.* **2009**, *131*, 144108.
(12) Stein, T.; Kronik, L.; Baer, R. *J. Am. Chem. Soc.* **2009**, *131*, 2818.
(13) (a) Neugebauer, J.; Gritsenko, O.; Baerends, E. J. *J. Chem. Phys.* **2006**, *124*, 214102. (b) Schipper, P. R. T.; Gritsenko, O. V.; van Gisbergen, S. J. A.; Baerends, E. J. *J. Chem. Phys.* **2000**, *112*, 1344.

(14) Gritsenko, O.; Baerends, E. J. *J. Chem. Phys.* **2004**, *121*, 655.
(15) Zhao, Y.; Truhlar, D. G. *J. Phys. Chem.* **2008**, *A 112*, 1095.
(16) Ziegler, T.; Seth, M.; Krykunov, M.; Autschbach, J. *J. Chem. Phys.* **2008**, *129*, 184114.
(17) Ziegler, T.; Seth, M.; Krykunov, M.; Autschbach, J.; Wang, F. *J. Mol. Struct. THEOCHEM* **2009**, *914*, 106.
(18) Ziegler, T.; Seth, M.; Krykunov, M.; Autschbach, J.; Wang, F. *J. Chem. Phys.* **2009**, *130*, 154102.
(19) Ziegler, T.; Krykunov, M. *J. Chem. Phys.* **2010**, *133*, 074104.
(20) Cullen, J.; Krykunov, M.; Ziegler, T. *Chem. Phys.* **2011**, *391*, 11−18.
(21) Ziegler, T.; Krykunov, M.; Cullen, J. *J. Chem. Phys.* **2012**, *136*, 124107.
(22) Krykunov, M.; Grimme, S.; Ziegler, T. *J. Chem. Theory Comput.* **2012**, *8*, 4434.
(23) Hirata, S.; Head-Gordon, M. *Chem, Phys. Lett.* **1999**, *314*, 291.
(24) Slater, J. C.; Wood, J. H. *Int. J. Quantum Chem.* **1971**, *Suppl. 4*, 3.
(25) Slater, J. C. *Adv. Quantum Chem.* **1972**, *6*, 1.
(26) Ziegler, T.; Rauk, A.; Baerends, E. J. *Chem. Phys.* **1976**, *16*, 209.
(27) Ziegler, T.; Rauk, A.; Baerends, E. J. *Theor.Chim. Acta* **1977**, *43*, 261.
(28) Besley, N.; Gilbert, A.; Gill, P. *J. Chem. Phys.* **2009**, *130*, 124308.
(29) Gavnholt, J.; Olsen, T.; Engelund, M.; Schiøtz, J. *J. Phys. Rev. B* **2008**, *78*, 075441.
(30) Kowalczyk, T.; Yost, S. R.; Van Voorhis, T. *J. Chem. Phys.* **2011**, *134*, 054128.
(31) Ziegler, T.; Krykunov, M.; Cullen, J. *J. Chem. Theory Comput.* **2011**, *7*, 2485.
(32) te Velde, G.; Bickelhaupt, F. M.; van Gisbergen, S. J. A.; Fonseca Guerra, C.; Baerends, E. J.; Snijders, J. G.; Ziegler, T. *J. Comput. Chem.* **2001**, *22*, 931.
(33) Van Lenthe, E.; Baerends, E. J. *J. Comput. Chem.* **2003**, *24*, 1142.
(34) Vosko, S. H.; Wilk, L.; Nusair, M. *Can. J. Phys.* **1980**, *58*, 1200.
(35) Becke, A. D. *J. Chem. Phys.* **1993**, *98*, 5648.
(36) Lee, C.; Yang, W.; Parr, R. G. *Phys. Rev.* **1988**, *B 37*, 785.
(37) See S1 of the Supporting Information.
(38) See S2 of the Supporting Information.
(39) Pople, J. A.; Krishnan, R.; Schlegel, H. B.; Binkley, J. S. *Int. J. Quantum Chem.* **1979**, *Suppl.13*, 225.
(40) Fletcher, R. *Practical Methods of Optimization*; Wiley: NewYork, 1980; Vol. *1*, pp 110−120.
(41) Fischer, T. H.; Almlöf, J. *J. Phys. Chem.* **1992**, *96*, 9768.
(42) Ziegler, T.; Baerends, E. J.; Rauk, A. *Theoret. Chim. Acta (Berlin)* **1977**, *46*, 1.
(43) Martin, R. L. *J. Chem. Phys.* **2003**, *118*, 4775.
(44) Amos, A. T.; Hall, G. G. *Proc. R. Soc.* **1961**, *A263*, 483.
(45) Wang, F.; Ziegler, T. *J. Chem. Phys.* **2004**, *121*, 12191.
(46) Wang, F.; Ziegler, T. *J. Chem. Phys.* **2006**, *122*, 74109.
(47) Wang, F.; Ziegler, T. *Int. J. Quantum Chem.* **2005**, *106*, 2545.
(48) Mori-Sánchez, P.; Cohen, A. J.; Yang, W. *J. Chem. Phys.* **2006**, *125*, 201102.
(49) Zhao, Y.; Truhlar, D. G. *J. Chem. Phys.* **2006**, *125*, 194101.
(50) Zhao, Y.; Truhlar, D. G. *Theor. Chem. Acc.* **2008**, *120*, 215.
(51) A few excitations in ref 33 have been reassigned in the present work leading to new excitation energies in the present study.